High Elevation Light Intensity Observation System V

Final Science Report

Dawson Beatty, Emma Cooper, Haleigh Flaherty, Joseph Frank,
Daniel Green, Ross Kloetzel, Alex Mulvaney, Virginia Nystrom,
Samantha Palma, Erin Shimoda, Colin Sullivan, Logan Thompson

University of Colorado at Boulder
Colorado Space Grant Consortium
Faculty Advisor: Brian Sanders

Figure 1: Picture of HELIOS during Day-In-The-Life testing

Contents

Nomenclature

ADCS	Attitude Determination and Control Systems
Ca-K	Calcium-K
CDH	Command and Data Handling
COSGC	Colorado Space Grant Consortium
DITL	Day in the Life
EPS	Electrical and Power Systems
FBD	Functional Block Diagram
FOV	Field of View
H-α	Hydrogen-Alpha
ND	Neutral Density
SBO	Sommers-Bausch Observatory

I. Mission

A. Overview

The objective of HELIOS V was to utilize the successful tracking system of HELIOS IV to track and take pictures of the Sun in the Hydrogen-Alpha (H-α) wavelength. HELIOS V was designed as a payload on the High Altitude Student Platform and was a continuation of the previous four HELIOS missions. The HELIOS V team built on the systems of HELIOS IV and added new optical science instruments to achieve high quality images of the Sun.

Mission Objectives:

1. Take advantage of the successful HELIOS IV system to gather science data.
2. Capture images of the Sun in the Hydrogen-Alpha wavelength.

B. Mission Background

1. High Altitude Balloon Observation

Currently the majority of solar observation is done either from ground based telescopes or orbiting space telescopes. These methods both have their drawbacks. Ground based systems have to deal with atmospheric interference, limiting the quality of observations or necessitating complex and expensive adjustments to account for this interference. Orbiting space-based telescopes operate without this atmospheric interference, but are extremely expensive to build and put into orbit. This severely limits the quantity of solar imaging missions in space. With these restrictions in mind, an alternative method to observe the Sun is through the use of high altitude balloon observatories. Solar observation from a high-altitude balloon platform such as the HASP platform has the advantages of being above 99.5% of the atmosphere to reduce interference, while also being orders of magnitude less expensive than a space-based satellite.

The Colorado Space Grant Consortium (COSGC) at the University of Colorado, Boulder (CU) has a history of high altitude observatory experiments. DIEHARD (2008) determined the viability of high altitude observatories by collecting diurnal and nocturnal images of celestial bodies to determine atmospheric turbulence and light intensity due to residual particles in the atmosphere. This was done using photometers mounted 45° from the horizon. BOWSER (2009) further determined the practicality of high altitude observatories by examining certain wavelengths of cosmic light and took corresponding diurnal images and light intensity readings of the sky. BOWSER also measured platform stability in order to determine the conditions in which future HASP missions will fly. SPARTAN-V (2010) worked towards the goal of supporting precise photometry from balloon based pointing systems and telescopes. SPARTAN-V focused on characterizing atmospheric scintillation and extinction to support the practicality of observing exoplanets from a high altitude balloon.

In 2012, a team from COSGC and CU Boulder flew HELIOS I, a mission to test the viability of solar observation from a high-altitude balloon platform. The mission was mostly optics driven with two cameras designed to take pictures of the Sun in H-α and Calcium-K (Ca-K) wavelengths. The HELIOS II and III teams then improved upon this design in 2013 and 2014 by flying a similar mission that was more focused on the ADCS. Both payloads had several issues, prompting a HELIOS IV mission designed to improve upon them both and track the Sun consistently. HELIOS IV was focused only on the engineering mission of tracking the Sun and not on its science mission, allowing for more time and effort to be dedicated to creating a robust tracking system. HELIOS IV functioned nominally throughout flight, tracking the Sun consistently and taking an equivalent science image once every two seconds on average, thus proving the viability of solar observation on a high altitude balloon platform.

2. Science Background

HELIOV V sought to take advantage of the robust system developed by past HELIOS teams to take high quality images of the Sun in the H-α wavelength, and thus fulfilling the long term goal of the HELIOS mission. As HELIOS IV did not encompass a true optical system, HELIOS V's optics were based off those of HELIOS III, which took telescopically magnified images of the Sun in the H-α wavelength. In addition to this, while HELIOS V initially proposed the implementation of a star tracker instrument in association with Colorado Space Grant Consortium's PolarCube project, the instrument was not flown due to budget issues with the PolarCube team.

C. Concept of Operations

The Concept of Operations (CONOPS) for the HELIOS V mission is depicted in Fig. 2. This CONOPS was based off of the initial predicted flight date of August 29th with a 7:00 AM launch time. The payload would be turned on prior to launch in order to collect data throughout ascent and into the float time. Float would be the optimal tracking period for the payload. Once the Sun set, the two cameras and tracking of the payload would be turned off to save storage space. The payload would not be completely powered down in order to keep the motor drivers on and therefore help keep the payload warm. This would be done in case the flight lasted pasts sunrise, allowing HELIOS V to have another tracking period. By keeping the payload on, it would stop it from getting too cold to power back on in the morning.

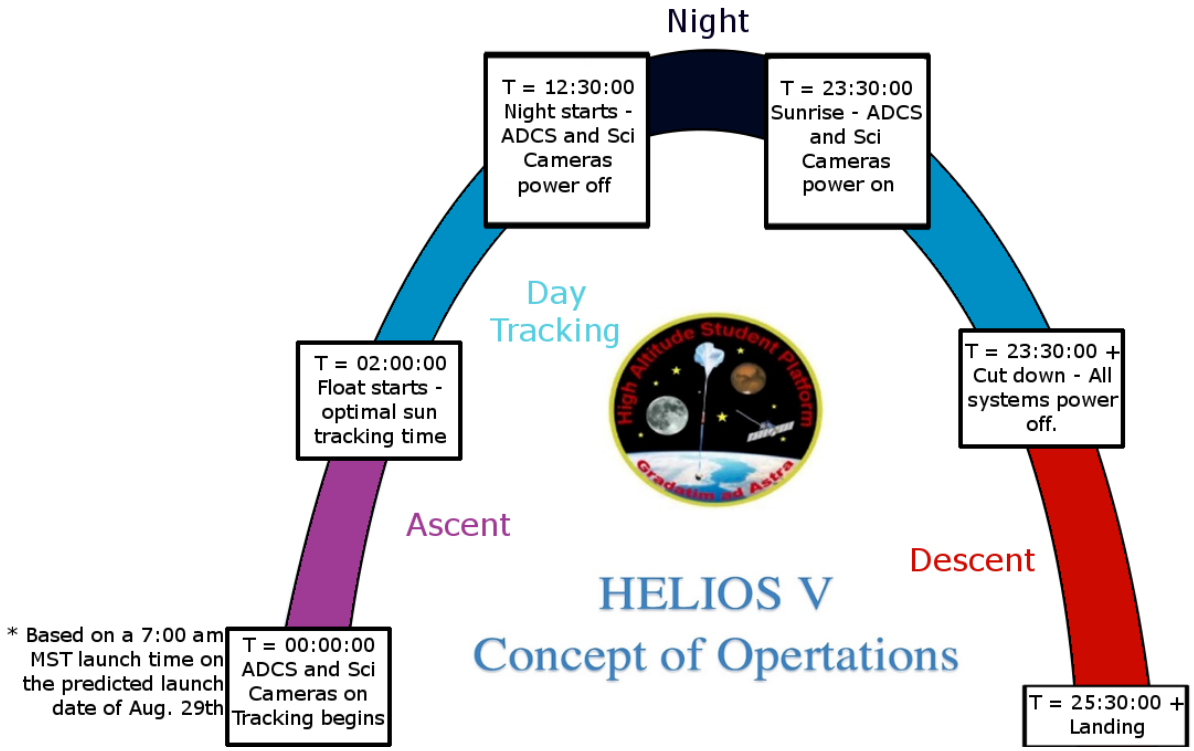

Figure 2: Concept of Operations

II. Mission Requirements

Level	Requirement	Derived
0	High Elevation Light Intensity Observation System (HELIOS) V shall have an optics system for capturing images of the Sun	
1	HELIOS V shall utilize the HELIOS IV system to locate the Sun and orient the optics system towards the Sun on-board a HASP flight	

Level	Requirement	Derived
0.1	The HELIOS IV upper housing shall be redesigned to be able to house any future solar observation instrument(s)	0
0.2	An optics system shall be designed and implemented to capture images of the Sun in Hydrogen-Alpha wavelength	0
0.3	A high altitude balloon solar observation system shall be designed and implemented and shall utilize the HELIOS IV payload and its tracking system for a COSGC-sponsored HASP flight	0

Level	Requirement	Derived
0.1.1	The camera housing shall be physically large enough to hold any future solar observation instrument(s)	0.1
0.1.2	The camera housing shall contain the HELIOS IV ADCS Camera system	0.1
0.1.3	The camera housing shall accommodate the HELIOS IV photodiode housings	0.1

Level	Requirement	Derived
0.2.1	The CDH system shall allow for storage of captured images	0.2
0.2.2	The primary science camera of the optics system shall have a field of view no larger than 1.5° x 1°	0.2
0.2.3	The primary science camera system shall fly a Hydrogen-Alpha filter with a maximum bandwidth of 5 nm	0.2
0.2.4	The primary science camera system shall have a resolution (plate scale) equal to or smaller than the minimum angular resolution	0.2
0.2.5	The optics system shall be insulated and isolated from all other systems' thermal footprint	0.2
0.2.6	The optics system camera shall be compatible with the optics CPU.	0.2

Level	Requirement	Derived
0.3.1	HELIOS V shall comply with all HASP requirements outlined by the Call for Proposals and other LaSPACE documents	0.3
0.3.2	HELIOS V shall comply with all budget and schedule constraints dictated by COSGC and HASP	0.3
0.3.3	HELIOS V shall maintain a proper operational environment throughout flight	0.3
0.3.4	HELIOS V shall utilize the ADCS of HELIOS IV	0.3

Level	Requirement	Derived
0.1.2.1	The changes to the HELIOS IV camera housing shall not interfere with the functioning of the HELIOS IV ADCS camera system	0.1.2
0.1.3.1	The changes to the HELIOS IV camera housing shall not interfere with the functioning of the HELIOS IV photodiodes	0.1.3

Level	Requirement	Derived
0.2.2.1	The optics system shall have one camera with a resolution of greater than 1280 pixels x 720 pixels	0.2.1
0.2.3.1	The optics system shall remain below 60 °C throughout the flight	0.2.3

Level	Requirement	Derived
0.3.1.1	Payload volume shall not exceed 38x30x30 cm	0.3.1
0.3.1.2	Payload shall resist the effects of up to 10 g vertical force and 5 g horizontal force	0.3.1
0.3.1.3	Payload shall utilize a twenty-pin EDAC 516 interface to HELIOS IV system power and analog downlink channels	0.3.1
0.3.1.4	Payload shall not draw more than +30 VDC or 2.5 A and shall split the provided +30 VDC to voltages necessary to operate payload	0.3.1
0.3.1.5	Payload shall allow serial downlink functioning at 4800 baud	0.3.1
0.3.1.6	Serial up-link shall allow for 2 bytes per command	0.3.1
0.3.1.7	Payload shall use a DB9 connector, RS232 protocol, with pins 2, 3 and 5	0.3.1
0.3.1.8	Payload shall transmit payload status to the HASP serial downlink	0.3.1
0.3.1.9	Payload shall be mounted according to the HASP platform interface requirements	0.3.1

Level	Requirement	Derived
0.3.2.1	All receipts and proofs of purchase shall be retained	0.3.2
0.3.2.2	Schedule shall include weekly deadlines for each phase of design, assembly, and integration process	0.3.2
0.3.2.3	Schedule shall include all design document revisions; including relevant presentations	0.3.2
0.3.2.4	Schedule shall contain weekly team meetings	0.3.2

Level	Requirement	Derived
0.3.3.1	The optics system structure shall be insulated to minimize thermal footprint of other systems	0.3.3
0.3.3.2	All systems shall remain within operating temperatures while experiencing external temperatures between -80 and 60 °C	0.3.3

III. Design

A. Design Overview

As shown in Fig. 3, the major components on HELIOS V are the telescope and science camera, which take pictures of the Sun in the H-α wavelength; a pair of photodiodes, to perform coarse tracking of the Sun in the azimuth direction; the ADCS camera, which takes pictures to enable the fine tracking of Sun; two Raspberry Pi's, which handle the software; two motors which enable HELIOS to move in the azimuth and elevation directions; and the EPS board, which communicates with and powers the system. HELIOS V is broken up into five subsystems: Structures, Optics, ADCS, CDH, and EPS. These subsystems will be detailed in the following sections.

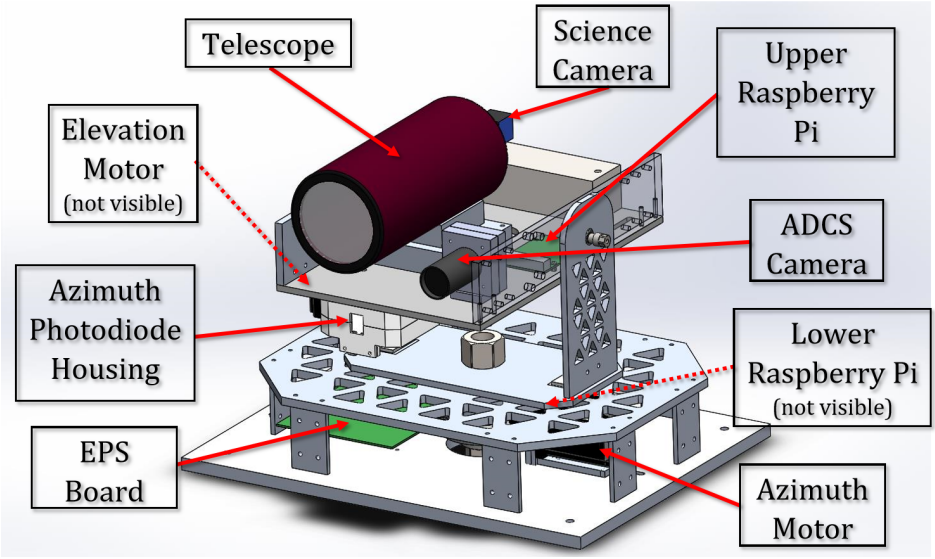

Figure 3: Major components of HELIOS V

B. Structures

1. *Lower Housing*

The base plate is a half-inch thick plate of 6061-T6 Aluminum. The plate is quite thick, allowing it to act as a heat sink for electronic components. The lower housing Raspberry Pi 2 and the PCB board are attached to the plate using standoffs. The azimuth motor is also fastened to the base plate, but lies on a thick aluminum shim. This elevates it to the proper position to mesh with the teeth on the dial gear of the axle sub-assembly. Eight rectangular support columns connect the top plate of the lower housing to the base plate using 4-40 screws. Lightening cuts have been added to the top plate for weight reduction. The axle assembly is suspended from the top plate by a flanged aluminum sleeve, which is secured to the top plate by six 8-32 screws and nylocks. Residing in the sleeve are two bearings around the motor shaft with an aluminum spacer in between the bearings. The central shaft is threaded at each end to allow inch and a half wide nuts to attach at both ends. The lower of these two nuts holds the dial gear in place, while the upper one fastens the motor to the rotary plate, allowing rotation of said plate. In addition, the shaft is hollow so that wires can be connected between the upper and lower housings without the rotation of the upper housing causing damage to the wires. The assembly is shown in Fig. 4.

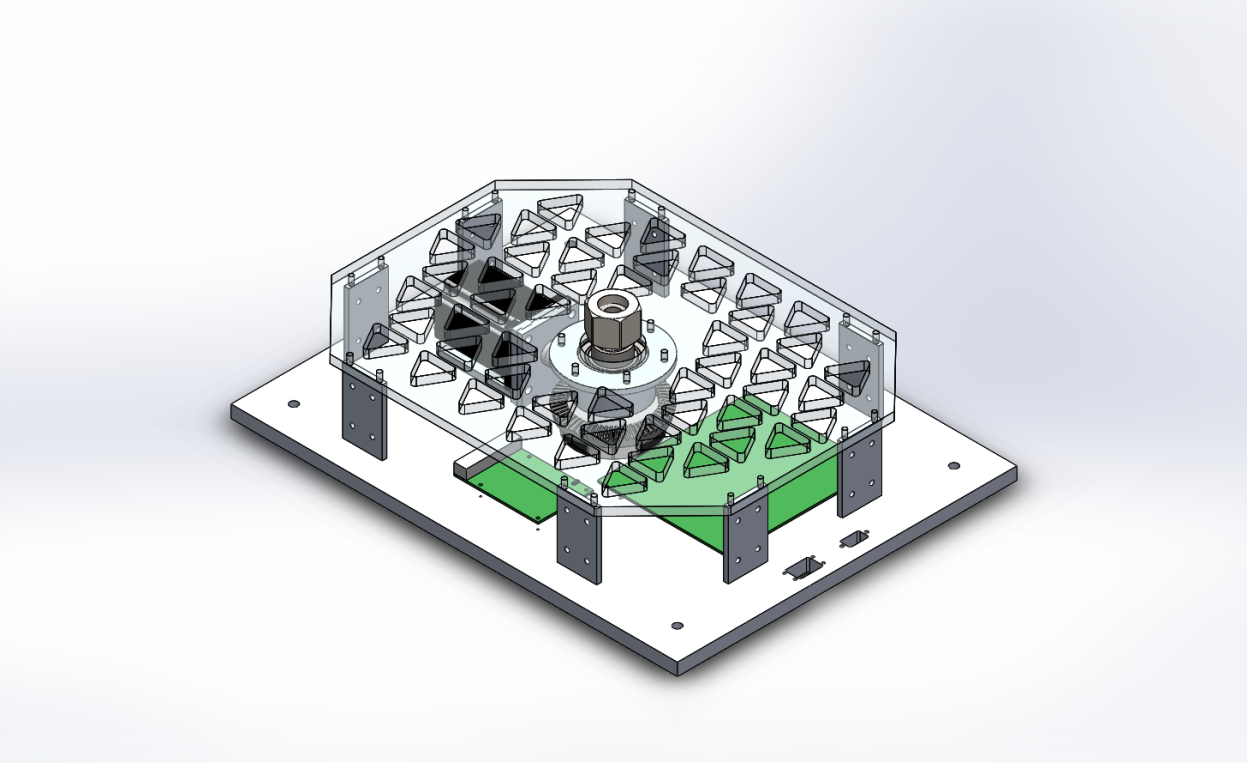

Figure 4: Lower Housing Assembly

2. Middle Housing

The rotary plate is a quarter inch thick rectangular plate of 6061-T6 Aluminum with its edges chamfered to reduce weight and the danger of sharp edges. Two plates with lightening cuts attach to the plate and support the upper housing. These walls are attached to the rotary plate by gusseted L-brackets with 8-32 screw and nut fasteners. The elevation motor is attached to one wall with two 6-32 screws and two dowels pins for support. The helical gear upon the elevation motor meshes with an identical gear on the upper housing in order to rotate the upper housing. On the same wall, the elevation motor limit switch is epoxied at a 60 degree angle. The switch ensures the upper housing cannot rotate into the rotary plate while the optics system tracks the Sun upwards. The assembly is shown in Fig. 5.

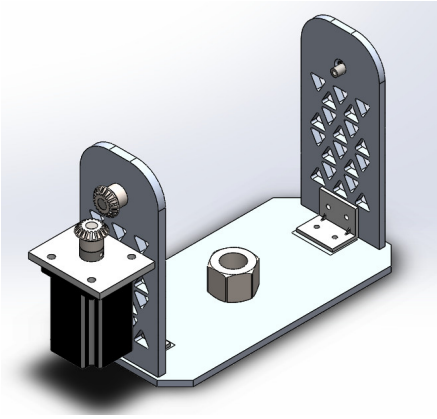

Figure 5: Middle Housing Assembly

3. Upper Housing

The bottom plate of the upper housing is a quarter inch thick plate of 6061-T6 Aluminum, the same material as all other plates. Two side plates act as walls for the upper housing, with each wall having a flanged bearing at its center. One wall has a drive shaft through its bearing which connects to a helical gear, and that gear in turn meshes with the elevation motor's gear to rotate upper housing. The drive shaft is a single 10-32 screw threaded through the helical gear and side wall. It is epoxied to said side wall to ensure it can not freely rotate with respect to the wall. On the other side wall is an axle shaft, ensuring that the upper housing is supported on both sides as it rotates. This shaft is fastened to the wall with a 10-32 screw threaded through the shaft's hollow center.

Attached to the under side of the upper housing bottom plate are the azimuth photodiodes, residing within their 3-D printed housing. This housing is attached to the bottom plate by four 1/4-20 screws and nuts. Additionally, the upper housing holds the upper Pi, fastened to the bottom plate with four aluminum standoffs. The ADCS camera is located at the front of the upper housing, fastened through a hole and radial slot by two 1/4-20 screws. A radial slot was implemented to allow the rotation of the camera for alignment with the science camera.

Beside the ADCS camera is the telescope resting on its mount. The two pieces of the Aluminum telescope mount connecting the telescope to the upper housing are attached to one another with four 6-32 screws threaded directly into the upper half of the mount. The mount attaches to the upper housing using four 8-32 screws which pass through two slots milled across the upper housing and fastened on the other side with nuts. These two slots allow for the translation of the mount, and therefore the telescope, for alignment purposes. The telescope mounts to its base with two M4x0.5 screws threaded through its outer shell. These screws are short as to not pierce through the telescope shell and into the interior of the telescope. The science camera fastens to the back of the telescope with a lens mount to retain concentricity between the two parts. With all the camera hardware to the front of the upper housing, a 2.4 kg counter weight is attached to the back half of the upper housing with two 1/4-20 screws passing through two slots, and fastened by nuts. The slots allowed for the counter weight to be translated towards or away from the center of the upper housing. Once balance was tested, the counter weight was fastened into place. The assembly is shown in Fig. 6.

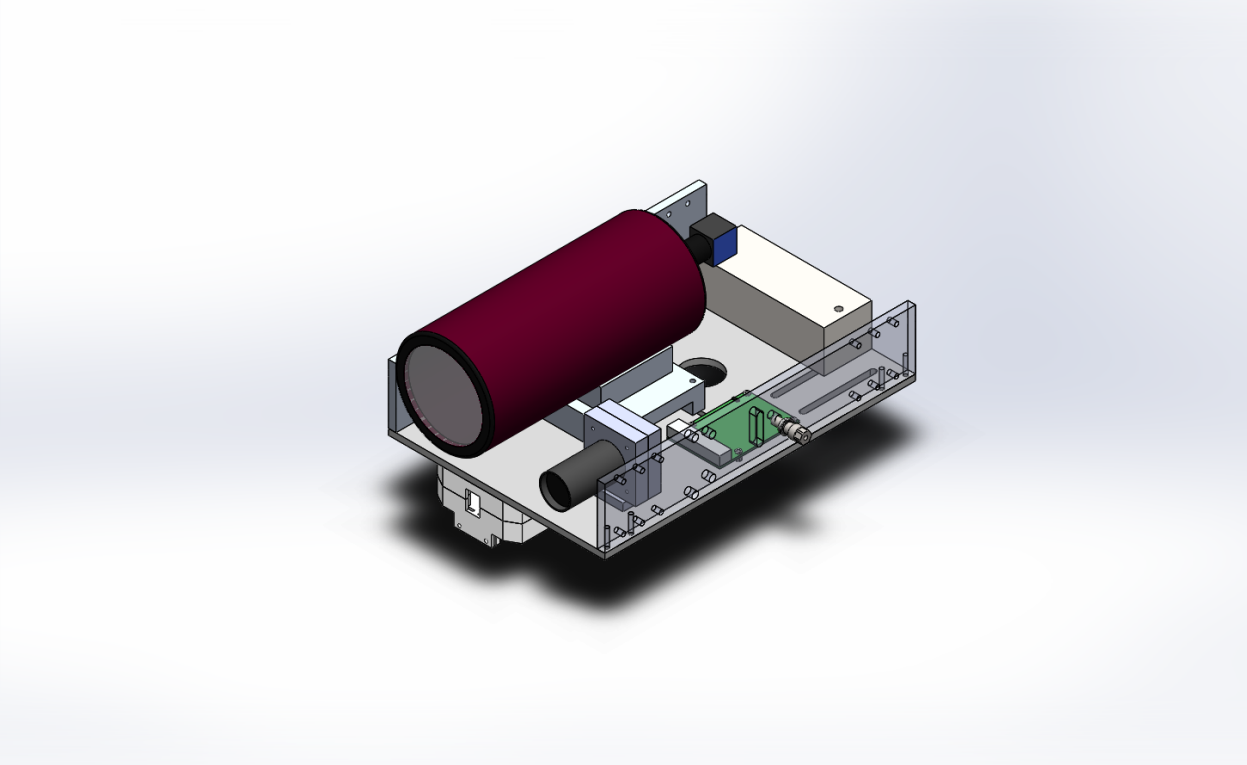

Figure 6: Upper Housing Assembly

4. Thermal

The motor drivers attached directly to the lower housing base plate to diffuse the large amount of heat they create.

To reduce heat into the payload due to the Sun's radiation, the lower housing base plate, lower housing top plate, middle housing rotary plate, middle housing support walls, upper housing side walls, and front edge of the upper housing bottom plate were painted white. In addition, MLI wraps were applied to three

locations on the payload. A strip wrapped around the support columns of the lower housing to protect the electronics in the lower housing. A sheet was attached to the underside of the top plate due to the holes the lightening cuts added in this design iteration. Finally, two MLI sheets were formed over the upper housing, with holes at the front from which the ADCS camera and telescope lenses protrude. The MLI is shown in Fig. 7.

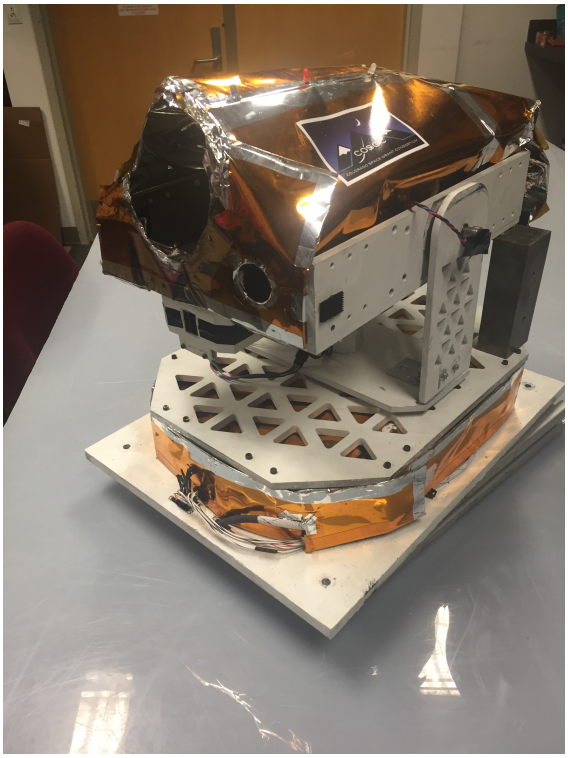

Figure 7: MLI in Position on HELIOS V

C. Optics

1. Optics System Overview

The primary goal for the Optics subsystem was to prove that better images of the Sun can be captured in the stratosphere than on the surface of the Earth. The overall design is based off the optical design of HELIOS III, which was the last HELIOS mission to fly an Optics system. The Optics subsystem comprises of two top-level components: the science camera and the ADCS camera. The science camera was able to capture telescopically magnified images of the Sun in the H-α wavelength with a small FOV for optimal image resolution. The ADCS camera was able to capture low magnified images of the Sun in the visible spectrum with a large FOV for optimal ADCS tracking.

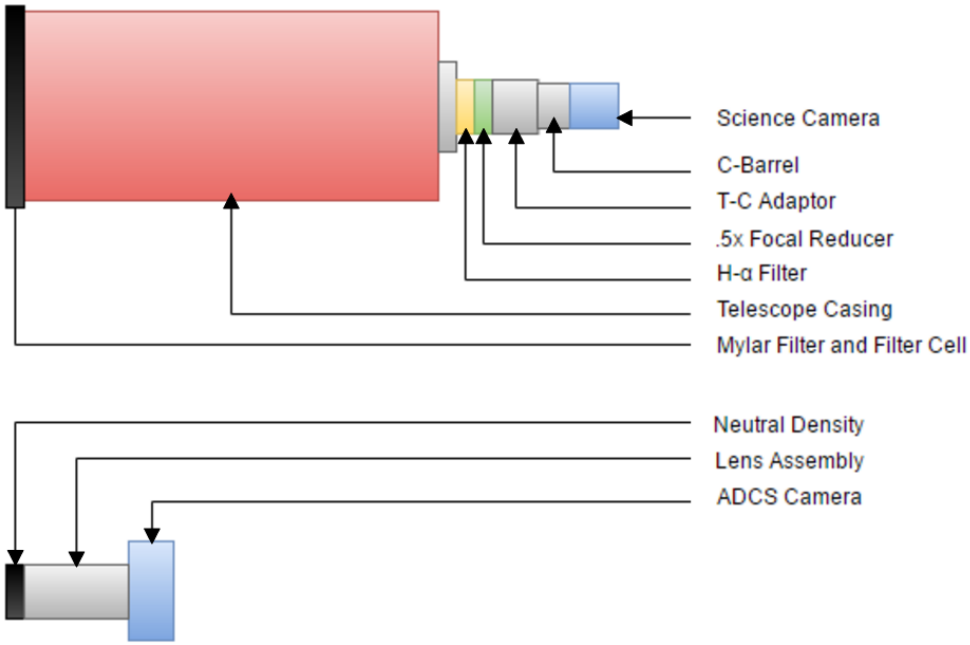

Figure 8: Optics System Overview

2. Components of the System

a. Ideal Wavelength

Past HELIOS missions have worked with both the H-α and Ca-K wavelengths, so for HELIOS V the Optics team needed to decide while wavelength to focus on. The Ca-K wavelength had potential as it showed the magnetic activity of the Sun and the wavelength had a better possible angular resolution than the H-α wavelength. The Optics team decided against the Ca-K wavelength though as it was less researched in the past HELIOS missions and the hardware purchased during the HELIOS III mission may not have worked for the Ca-K wavelength. H-α also offered more benefits and less risks than Ca-K. H-α would show solar features such as sunspots and solar flares, which would be more easily distinguished with a small telescope system. It had been thoroughly researched by the HELIOS teams and the only major drawback of H-α was the financial limitations on hardware. In the end the team decided that the financial limitation would be worse for the Ca-K hardware because it would require all new equipment, instead of H-α which the previous HELIOS teams had already purchased several parts for.

b. Camera

At the beginning of the HELIOS V project, the team already had a camera that was purchased during the HELIOS III mission. This was an Image Source, DMK 51BU02.H industrial camera from 2013. As the Optics team began to work with the camera though, they ran into several problems. The main issues were with the resolution of the camera and the software it used. The camera only had an 8-bit resolution and the outdated software was causing compatibility problems for the CDH team.

The team began looking for a new camera, staying within Image Source since the basic code to use their cameras was already set up. When considering a new camera, the team wanted to ensure it had at least 12-bit resolution, had a charge-couple device (CCD) sensor chip, and the same or larger chip size as the DMK 51BU02.H. After extensive research into the many options, the team selected the DMK 23U274. The DMK 23U274 met all of the desired specifications, and had the bonus factor of being more compact than the DMK 51BU02.H. For these reasons, the Optics team elected to replace the old camera with the DMK 23U274, which was successfully implemented and tested.

Figure 9: Camera Selection

c. Focal reducer

HELIOS V Optics incorporated a .5x focal reducer in its optical configuration, utilizing a positive lens to reduce the focal length of the system and thus increase the field of view. An increased FOV increased the likelihood of capturing an image of the Sun, but also introduced decreased resolution of solar features. Due to the Sun being smaller in the frame, the angular resolution of the Sun decreases, thus decreasing the quality of the image. Two options were originally proposed for HELIOS V's focal reducer. The first option was an Orion FR1 .5x focal reducer which was originally part of the HELIOS III design and was proven to work. The second option was an Astronomics .44x focal reducer which was originally included in the HELIOS V proposal, as it allows the system to capture a larger portion of the Sun. These focal reducers are summarized in in Tab. 2.

It is also important to note that while the Orion FR1 was easily implemented into the system, the non-standard size of the Astronomics focal reducer would make implementation extremely difficult.

Table 2: Focal Reducer Comparison

Focal Reducer	Magnitude	Price	Resulting FOV
Orion FR1	.5x	Already owned	.779°x .623°
Astronomics	.44x	$525.00	.886°x .708°

The Optics team decided to stay with the .5x Orion focal reducer after taking these factors into consideration. Although the filter would not allow for an increase in FOV, both the cost of the component and the challenge of implementing it into the system were prohibitive.

Figure 10: Orion Deluxe Safety Film Solar Filter

d. Solar Filters

Previous design iterations of HELIOS focused primarily on the use of a front, primary neutral density filter followed by a series of long-pass filters. These filters were used to minimize the intensity of light passing through the H-α filter, as well as minimizing the amount of magnified light that strikes the camera chip. Originally the HELIOS V Optics system proposed the use of a series of long-pass filters like those on past HELIOS missions. However, they were removed as it was discovered that the long-pass filters weren't entirely necessary to protect the system, and caused measurable image distortion. Instead, the HELIOS V Optics team utilized a front primary Mylar filter that will be discussed below along with the Orion .5x focal reducer, and the H-α filter as shown in Fig. 8.

In addition to other filters, past HELIOS missions have used a simple and inexpensive ND-10 gel filter to filter out 99.99% of visible light. While HELIOS V Optics had originally planned on using the same material, it was eventually traded out for a Mylar filter along with a filter cell as the team had trouble taking usable images with the ND filters used in the past. While this option cost significantly more than the ND-10 filters, it was necessary in the success of the Optics team. The team purchased an Orion Deluxe Safety Film Solar Filter, shown in Fig. 10.

3. Successful Image Criteria

a. Definition of a Successful Image

A successful image was defined as any image with at least 50 percent of the Sun. This criteria seemed achievable based on successful images taken during flight on HELIOS IV. Images with only a fraction of the Sun can still produce useful science data. With the chosen optics chain, the full disk of the Sun could not be fully captured.

b. Quantification of a Successful Image

The image being in focus was the second part of the successful image definition. To do analyze this, the Optics team needed a method to quantify the focus of an image. Assistant Professor Jason Glenn, one of the Optics team's mentors, introduced the team to the method of pixel plots. This method plots a row of pixels from an image as a series of values from 0 to 1, 0 for black and 1 for white.

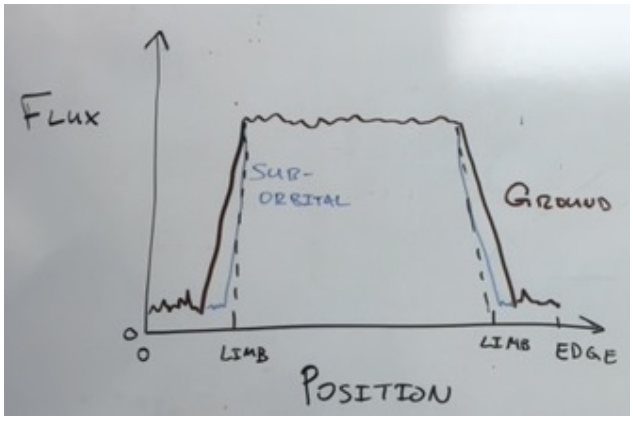

Figure 11: Pixel Plot Explanation

As seen in Fig. 11, the resulting plot has a plateau shape. The slope of the line before and after the plateau give a quantifiable measurement of image quality, as a sharper image would have a higher slope.

D. Attitude Determination and Control Systems

1. *Overall Design*

The Sun-tracking system on HELIOS V had two components: a coarse-tracking system and a fine-tracking system. The coarse tracking used photodiodes to find the Sun and guide HELIOS to center the Sun in front of the payload. The Attitude Determination and Control System (ADCS) camera accomplished the fine tracking, which took images of the Sun, analyzed them, and indicated how the payload should move to center the disk of the Sun in the pictures taken by the ADCS camera. This subsystem played an especially critical role with the addition of an optics system, since the science camera has a narrow field of view.

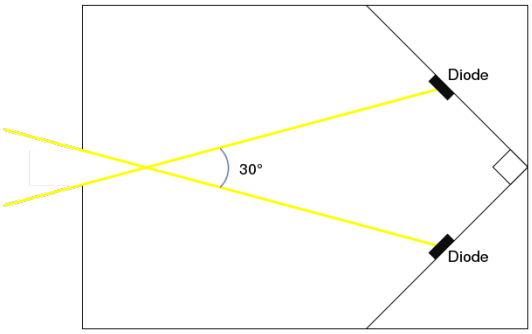

Figure 12: Interior of diode housing

HELIOS V differed from HELIOS IV in that only one pair of photodiodes were used. In the design of HELIOS IV, two sets of photodiodes were used for rough tracking on both the azimuth and elevation directions. Electrical problems with one set of photodiodes (as discussed later) necessitated a change in the tracking algorithm. The ADCS team decided to modified the tracking algorithm to use only one pair of photodiodes, as shown in fig 13.

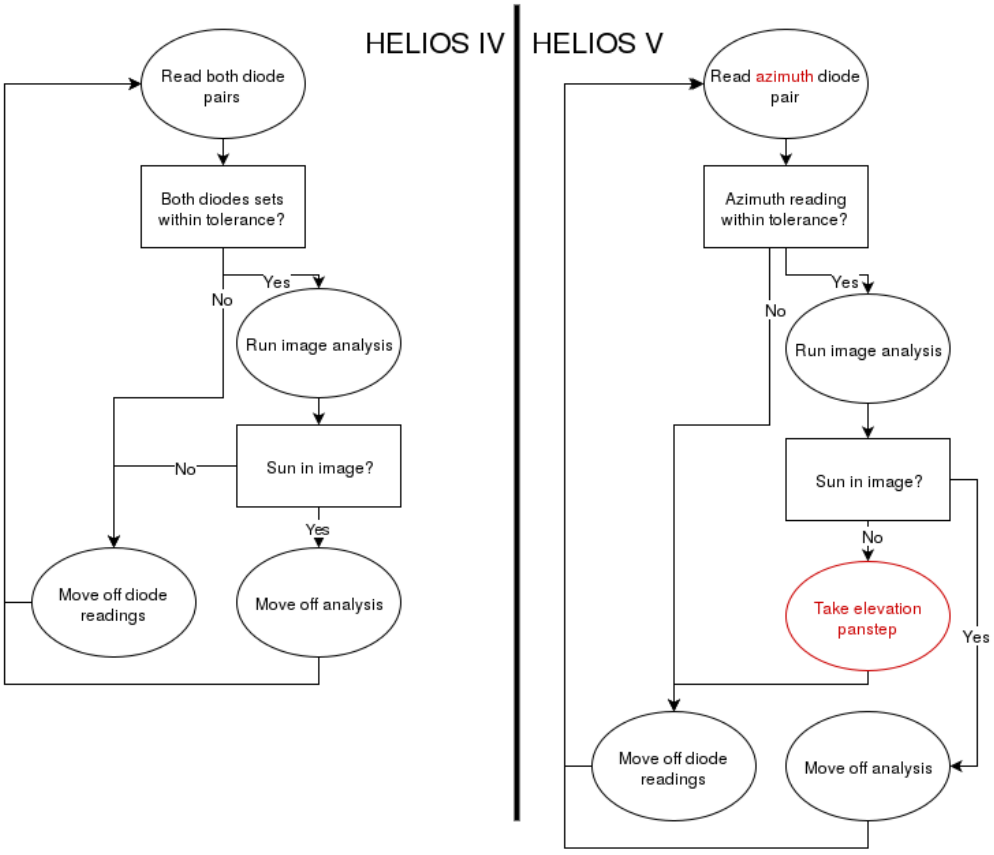

Figure 13: Sun-tracking algorithm. Changes from HELIOS IV shown in red.

HELIOS V used two photodiodes to find and center the Sun along the azimuth axis, then repeatedly panned up and down along the elevation axis until centering the Sun within the 22.9°x 17.2°field of view of the ADCS camera. With a 30°field of view through their encasement, the diodes sat at a 90°angle to

each other, meaning a perfectly centered Sun struck each diode at a 45°angle, as shown in figure 12. When the Sun was not centered, the light struck the diodes at different angles, leading to a difference in intensity. This difference in intensity was quickly calculated and the housing moved in a direction towards the Sun accordingly. Once the photodiodes had successfully brought the Sun within the ADCS cameras field of view, the camera took over and began fine tracking.

The ADCS flight loop constantly checked if the Sun was in the field of view of the ADCS camera. If so, the program defined the disk of the Sun and its distance to the center of the image, as seen in Fig. 14. Based on the location of the Sun, the loop determined and executed the appropriate steps with the motors to move the Sun closer to the center.

When the counterweight fell during the flight of HELIOS IV, the internal motor count was thrown off from true as well. To combat the possibility of this happening again, a limit switch was attached at the maximum inclination of the upper housing. Every time the payload panned up to its maximum, the motor count was re-zeroed. In addition to limiting the effect of mechanical failures, this change also mitigated the possibility of any elevation motor drift.

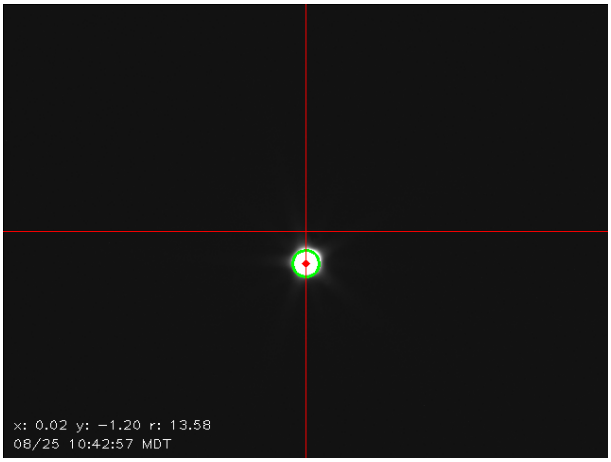

Figure 14: Fine tracking using ADCS image analysis. Distance from image center to Sun center shown in bottom left.

2. Diode Failure

On HELIOS IV, two pairs of diodes were used: one pair to respond to light in the azimuth direction and one pair to respond to light in the elevation direction. Because of the success of the HELIOS IV tracking system, the diodes were intended to be used by HELIOS V as well. However, the diodes broke during testing. The photodiode boards were unable to be reproduced and the elevation diodes had to be removed from the system. Because HELIOS V would be unable to track the Sun with only one set of diodes using the HELIOS IV tracking software, the tracking algorithm had to be changed in order to achieve mission success. The azimuth diode pair was retained rather than the elevation pair because HELIOS V had a greater range of motion in the azimuth direction than the elevation direction. It is therefore more difficult for the ADCS camera to capture the Sun in the azimuth direction than in the elevation direction.

E. Command and Data Handling

The CDH system aboard HELIOS V was responsible for communications with the HASP platform, and collecting and managing data from the Optics, EPS, and ADCS subsystems. The CDH system utilized two Raspberry Pi 2 devices, and flight code written in Python. Previous HELIOS missions flew a single Raspberry Pi 2 in the lower housing. The second Raspberry Pi 2 was a new addition, which was placed in the upper housing to help with the increased processing necessitated by the science instrument. Each Raspberry Pi had several loops running at the same time, separated for simplicity into distinct Python control threads.

1. Lower Pi – ADCS Thread

The ADCS thread ran all of the Sun tracking code for the mission. This included running the tracking algorithm main loop six times per second, recording status messages, and taking an image such as the one seen in Fig. 14 every ten seconds.

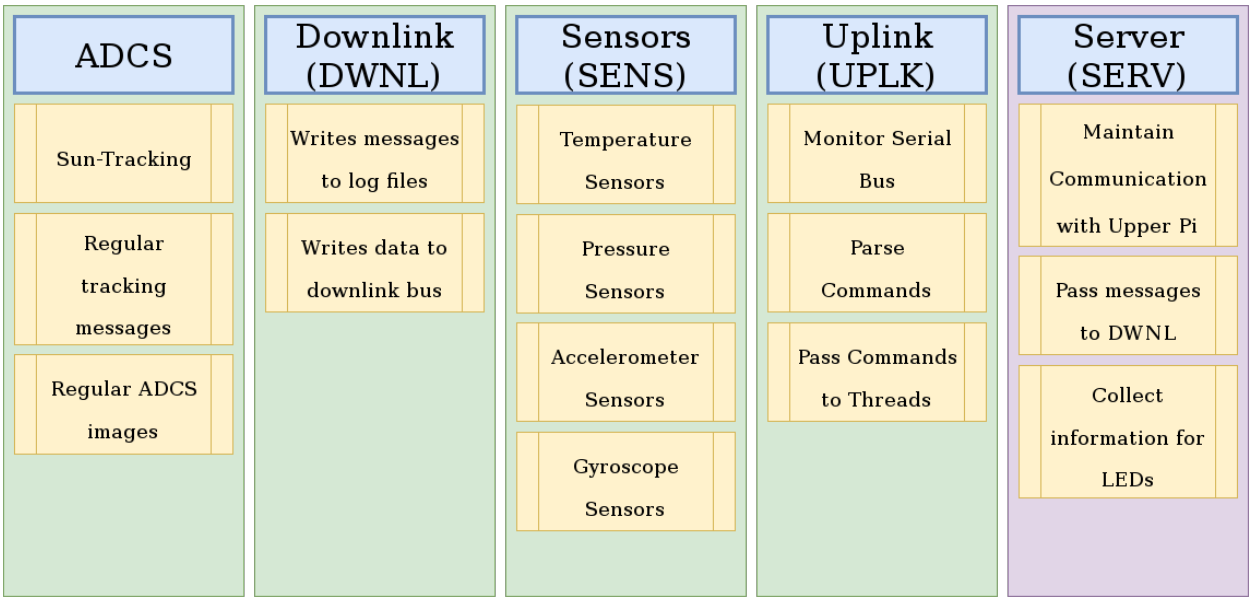

Figure 15: Diagram showing Python threads running on the Raspberry Pi 2 in the lower housing. Threads reused from HELIOS IV shown in green, new thread shown in purple.

2. Lower Pi – Downlink Thread

The Downlink thread managed all information that needed to be sent to the ground over the serial bus, as well as all messages to be logged. Whenever another thread had another piece of information to be logged or sent to the ground, the thread added it to a queue which the Downlink thread regularly read off. Each thread had its own separate log kept by the Downlink thread for ease of analysis and debugging.

3. Lower Pi – Sensors Thread

The Sensors thread managed reading and recording of all the atmospheric sensors on-board the payload. This included temperature, pressure, accelerometer, and gyroscopic sensors. In total, 14 temperature sensors were used, placed on key components of the payload and outside to record ambient temperature. A reading of each of these sensors was taken once every ten seconds, then passed to the Downlink thread to be recorded and sent to the ground.

4. Lower Pi – Uplink Thread

The Uplink thread acted as the counterpart to the Downlink thread; all messages sent up from the ground passed through the Uplink thread for handling. The thread constantly monitored the serial bus, and appended the command to its target thread's command queue for handling in the thread. This included commands directed to the Upper Raspberry Pi, which needed to pass through the Server thread first.

5. Lower Pi – Server Thread

The two Raspberry Pis maintained a Transmission Control Protocol (TCP) link over an Ethernet cable for the duration of flight. The Server thread initialized and maintained this link. The implementation of a basic communication protocol between the two Pis was inspired by the OpenSSL "Heartbeat" extension. Every 5 seconds, the Server thread sent a simple message to the Upper Raspberry Pi, including commands if any had been received from the Uplink thread. Before each of these messages, the temperature readings from the temperature sensors was checked, and a warning was sent if the value was too high.

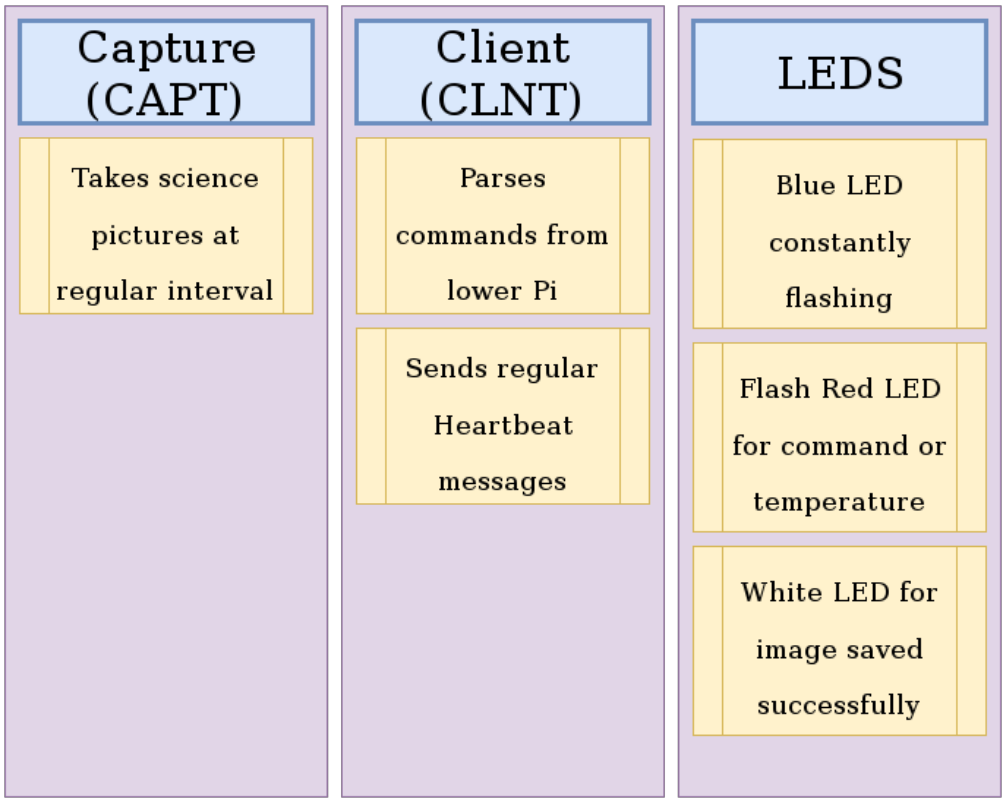

Figure 16: Python threads running on the Raspberry Pi 2 in the upper housing. All threads needed to be written for this mission, as HELIOS IV only flew one Pi.

6. Upper Pi – Client Thread

On the other side of the Ethernet cable, the Client thread monitored the connection with the Server thread. The Upper Pi knew to expect a message every 5 seconds, and attempted to reconnect if no message had been received for 15 seconds. If a warning or command was present in the message, the command was passed to the target thread, and the warning passed to the LED thread.

7. Upper Pi – Capture Thread

The Capture thread's only task was to take images through the science camera at a predefined rate, and save them to the Micro SD card. Commands from the ground could change the exposure time or capture rate.

8. Upper Pi – LEDs Thread

The LEDs thread existed to control the health and status LEDs mounted on the top of the payload. The blue LED normally flashed at a constant rate to show that the payload was on, and adopted a slower flash during night mode. The red LED flashed three times when any command was received from the ground, and constantly flashed at a fast rate if the payload began to overheat. The white LED flashed after a science image was confirmed as being saved.

F. Electrical and Power Systems

1. Board Design

There was one main power board, which took in power from the HASP platform and used a pair of buck converters to convert the 30 V given by HASP to the appropriate voltages for the components as described in the Power Budget in Table 3. It also took the telemetry line from HASP to the Raspberry Pi, which facilitated communication between HELIOS and HASP. The board brought power and data to all components of the subsystem as described in the Functional Block Diagram in Fig. 17. The power board on HELIOS V was the same board as used on HELIOS III and IV. The board functioned nominally on both flights and was deemed to be in good working condition. The schematics in Appendix B describe the board design.

2. Electronics Functional Block Diagram

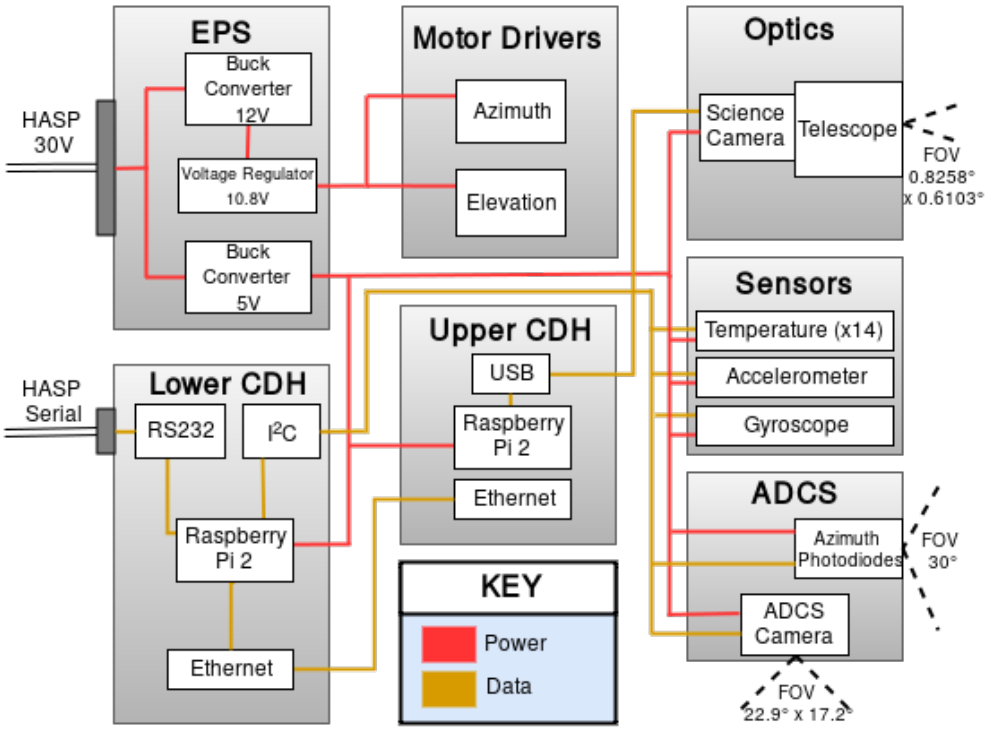

Figure 17: Electronics flow

3. Power Budget

The components on HELIOS that consumed significant power are listed below in Table 3. All other sensors consume negligible wattage. Even at maximum operation, HELIOS consumed below the HASP limit of 75 W and 2.5 A. At typical operation at 30 V, HELIOS consumed about .75 A and 22.5 W.

Component	Voltage (V)	Current (A)	Power (W)
Raspberry Pi 2	5.0	1.1	5.5
Raspberry Pi 2	5.0	1.1	5.5
Elevation Motor Driver	10.8	1.2	13.0
Azimuth Motor Driver	10.8	1.2	13.0
ADCS Camera	5.0	.75	3.8
Science Camera	5.0	2.5	12.5
Micro Switch	3.3	.33	1.1
Total Power	30.0	1.81	54.5

IV. Testing

A. Optics Testing

1. Heat Test

The goal of the heat test was to see how heat impacted the optics system, and in particular, the telescope. The maximum temperature to test the optics system at was chosen to be 50 degrees Celsius.The operating temperature of the camera was given by the manufacturer as 0 - 45 °C. A temperature was chosen slightly above this range to account for any possible error during flight that would cause the system to heat above this temperature range. To perform this test, a solar oven was created by forming a box without a lid using foam core. Saran wrap was used to cover the box to keep the more contained around the optics system. Four resistor heaters were placed inside the oven along the edges. Four temperature sensors connected to an Arduino were also placed inside to collect the temperature data during the test. The telescope was pointed at the Flatirons, a rock formation on the mountains next to Boulder, and images were taken to compare with the images taken during and after the heat test. The telescope was then placed into the solar oven and temperature data was recorded every 15 minutes. The telescope was taken out of the oven about once every hour, when it would then be used to take more images of the Flatirons. This process continued for four hours, and then the images taken during the test were compared to those taken before the test. The heat test was determined to be a success since there was no measurable impact on image quality by the heat.

Figure 18: Images during heating

2. Cold Test

The goal of the cold test was to see how cold temperatures impact the optics system, in particular, the camera's ability to operate. The lowest temperature to be reached during the cold test was chosen as -25 degrees Celsius, as this was the lowest temperature recorded during the flight of HELIOS IV. The freezer box, shown in Fig. 19, was used to perform the cold test. Once the optics system was placed in the freezer box, pieces of dry ice were placed around it. Fans connected to batteries inside the box were turned on to circulate the cold air. Temperature sensors were placed around the optics system to collect temperature data for the duration of the test. Once the desired temperature was reached, the camera was turned on and the quality of the image was assessed. This test was determined to be successful because the image quality of the camera was unchanged after the optics system was removed from the freezer.

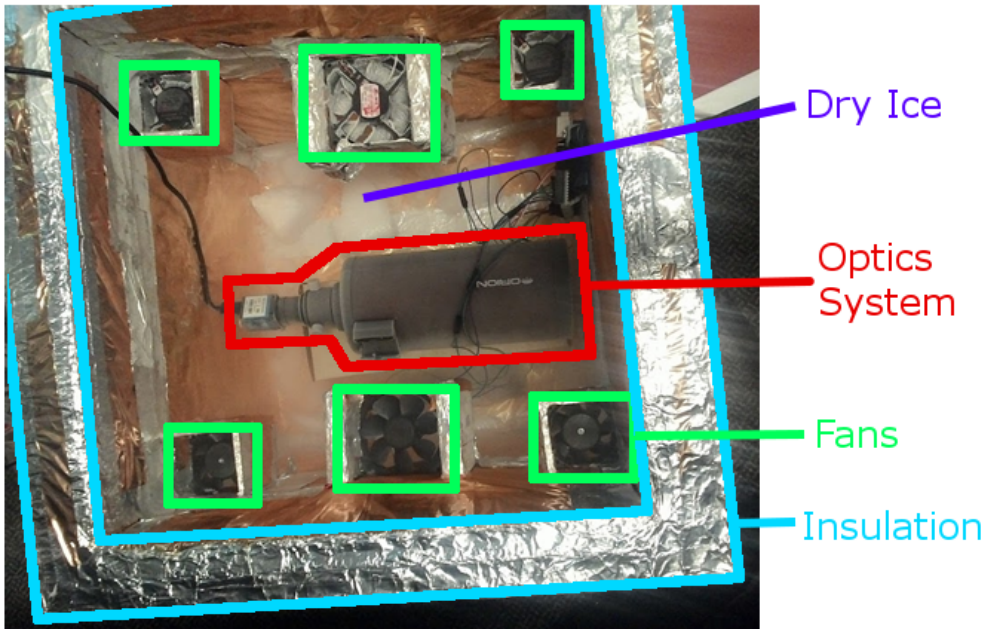

Figure 19: Cold test set up

3. Field of View Test

The goal of the FOV test was to confirm the FOV of the camera and make adjustments as necessary. This information would help the team know what images to expect during flight. For example, this test was able reveal how likely it is to capture an image with the full disk of the Sun. Equation 1 relates the distance between the lens and the focal plane (D), the reduction factor (R), and the focal length of the reducer (F).

$$D = F * (1 - R) \tag{1}$$

This equation was used to find an approximate initial position of the focal reducer that would optimize the FOV (around 47.5 mm with a focal length of 95 mm with the .5x focal reducer). Images were then taken with this configuration and the field of view was calculated from these images. From these calculations, it was determined whether or not the position of the focal reducer should be adjusted. This was done using a number of empty barrel attachments that would either lengthen or shorten the distance between the focal reducer and the camera chip. In addition to this, it was taken into account how easy the image was to focus and if any sort of lensing effects were present.

Figure 20: Image taken with field of view of .6402 x.4801

4. Exposure Test

The goal of this test was to determine the optimal exposure time for the science camera during flight. To find the optimal exposure time, the team first collected several images, and then processed their exposure level using histograms of their pixel values. An example of the range of values can been seen in Fig. 21.

To gather the images, the optics system was brought outside in its correct flight configuration, and was then pointed on the Sun. To start, the image exposure was set at a baseline exposure of .5 seconds and gain of 0. With this setting, five images of the Sun were taken and the exposure of the camera was lowered by .01 seconds.

This process was repeated until the image was indistinguishable from a black background. From this point, a histogram was created of pixel values across an image. The values of pixels across an image range from 0 to 2^{12}, denoting the upper dynamic range of the science camera. The goal was to take an image that had the peak of its pixel value distribution in the range of 40-70% of the maximum value, indicating that the image was not saturated, nor was it too dark to distinguish features on the Sun. This was balanced with trying to keep the signal to noise ratio at a minimum using the built in gain function on the science camera. A visual representation of the results can be seen in Fig. 21. Based on this test it was possible to conclude that an optimal exposure for the science camera would be between approximately .08 and .13 seconds. While these moderately long exposure values could possibly allow for pixel smearing as a result of platform slew, it was deemed acceptable based on accelerometer and gyroscope data from HELIOS IV and the pursuit of less noise on the images. An example of a properly exposed image from the test is shown in Fig. 22.

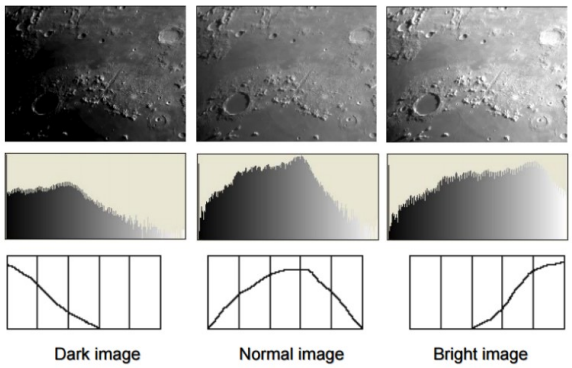

Figure 21: Visual Representation of Exposure Levels

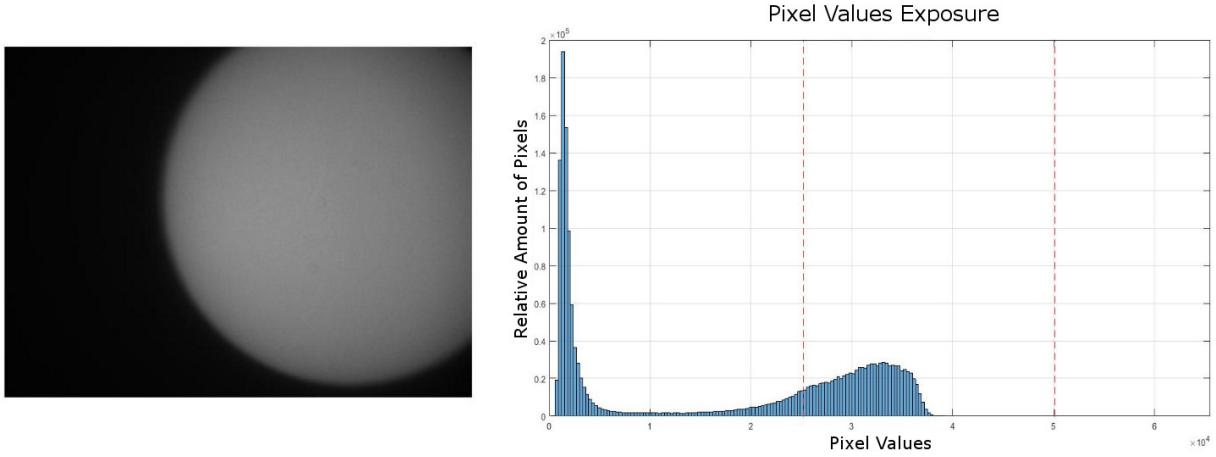

Figure 22: Successfully Exposed Sample Image and Plot

5. Alignment Testing

One of the most challenging parts of HELIOS V was the alignment of the two on-board cameras. It was mission critical that these cameras be aligned, but doing so by hand was difficult as it required the team to adjust the two cameras while the payload was trying to actively track the Sun. Even after aligning the cameras on the Sun, the Sun continued to move through the sky. The team went to the Sommers-Bausch Observatory (SBO) to work with director Fabio Mezzalira. SBO has several telescopes that can track the Sun, and the 24" SBO telescope was sturdy enough to mount the payload on top of it.

For the test, the team locked the payload in a stable, forward position using zip ties and gaffers tape. This way, the payload could not rotate independently of the telescope, therefore it was always facing the same direction as the SBO telescope. The payload was then mounted onto the SBO telescope, as seen in

Fig. 23, left. Both the science and ADCS cameras were connected to laptops to show live feeds from the cameras.

To start the test, the SBO telescope began tracking the Sun and the team adjusted the payload until the science camera had the Sun in the center of its field of view. Since the SBO telescope moves with the Sun, it keeps the Sun centered in the science camera's field of view for the duration of the test. The ADCS team then moved the ADCS camera until the Sun was in the center of its field of view as well. The team made sure to mark the correct locations for both cameras onto the base plate of the upper housing, as well as recording the residual offset to be corrected in code.

After this test, the cameras were aligned. Small adjustments were needed afterwards to fine tune the alignment, but the marked locations from the test allowed the team to correctly position the cameras each time.

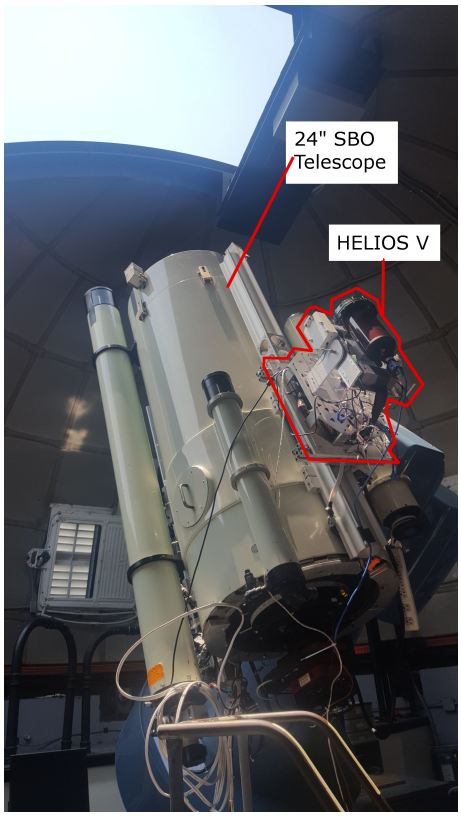

Figure 23: HELIOS V attached to the SBO telescope

B. Command Verification Testing

1. Summary

Three full Command Verification Tests were performed at different stages of development during payload buildup.

In each of the tests, all of the LED functions were verified as described in Section III-E-8. Each of the commands in the commanding list, seen in App. A, were sent to the payload to verify the command enacted the expected response.

2. Results and Changes

All three of the command verification tests were completely successful and verified expected functioning of the full CDH system. Despite these successes, the team felt apprehensive about sending commands except when a problem was obvious and needed intervention. Due to this, the system was designed to be able to function as autonomously as possible.

C. Systems Testing

1. Summary

Systems testing began in early June and continued through the end of July, providing a comprehensive evaluation of the entire payload. After all of the subsystems tested their individual components of the payload, the team integrated them together at the beginning of June. This initially led to problems since many of the subsystems did not function properly with the others, therefore system tests were designed to work out these bugs. In addition to this, the system tests attempted to simulate all possible situations that the payload could encounter, and ensure that the subsystems all respond in a cohesive and proper manner.

Due to the nature of the mission, all system testing needed to be conducted in the early morning to avoid the thunderstorms that plague Colorado afternoons. The payload would not respond well to any sort of cloud cover and it was especially important that the Sun was not too high in the sky (the payload can track no higher than 60°). The team would set-up HELIOS on a turntable, connect the payload to power and a monitor, and begin testing, as seen in figure 24. Small adjustments were made through the keyboard and monitor set-up with larger fixes occurring after testing was completed for that day.

Once the payload was powered on and the cameras were verified to be working, the test members would begin to rotate the payload in increments and watched how the payload reacted. This included 10°, 30°, 45°, 90°, 180°off the "zero" position facing the Sun. If the payload found the Sun in a smooth and timely manner, the team would move on to blocking the camera or photodiodes. This demonstrated the ability for the payload to react to shadows from the balloon, other payloads, or a lull in tracking. The payload was designed to continue to seek the Sun but refrain from drastic changes in position. System tests were concluded with a brief run-through of the commands, especially the nudges, once again to ensure the payload could find the Sun again.

Figure 24: Set-up of system testing

2. Results and Changes

The team conducted a total of twelve full system tests from June through July. As expected, there were many changes to be made, with the major changes highlighted in the table below. The tests were able to give the team a sense of what the system was capable of, as well as data to finalize the post-flight analysis procedure.

Problem	Sub-system	Solution
Elevation diodes not reading correctly	EPS	Remove elevation photodiodes, implement new tracking algorithm
Payload skips over Sun (ADCS camera not checked)	CDH	Increase diode tolerance to check ADCS camera, led to removal of elevation diodes
Improper balance causing elevation drift	Structures	Test balance and adjust counterweights
Shaky movement during tracking	Structures	Tightening motor nut, reduce step size, properly align and secure screws
Bugs in downlinking and data collection	CDH	Constant debugging

After conducting the six successful tests, with all major functions of the payload working and only minor bug fixes (if any), the team deemed that the payload was ready for Day in the Life Testing. The success of the tests became very clear when any attempt to "break" the tracking of the payload failed and the system was still able to focus on the Sun.

D. Day in the Life Testing

1. Summary

Day in the Life (DITL) testing of the full system began near the end of July. These lengthy tests were conducted to ensure that the payload could function for a duration similar to flight time. The tests began at sunrise in order to maximize daylight, and if weather permitted, the test would continue to track uninterrupted until sunset. Since the payload was not touched during the test, the test provided the team with data similar to that expected during flight.

DITL tests were conducted from the roof of the University of Colorado Engineering Center, in a location where no shadow would be cast on the payload. The weather was monitored at all times since any rain could cause permanent damage to the payload. The team would then set-up the payload with a power source and monitor, turn the payload on and watch it track for fourteen hours.

2. Results and Changes

Two DITL tests were conducted with the fully integrated payload, one on July 14 and the other on July 21. Most of the changes from the DITL tests dealt with the tracking algorithm and where the ADCS camera was centered. It was clear when the payload was not on the Sun, and some trends in the location the camera tracked to were noticed and fixed.

The first day in the life test ran from 6:30 AM to 8:30 PM, a full fourteen hour period. During this time, the payload was able to track through the time when the Sun was out of the field of view (around mid-day), from one horizon to the other. The tracking and focus of the cameras were proper, however only 32 GB of science images saved due to a data storage allocation issue. This was quickly resolved. Unfortunately, all of the science images were deleted following the test when a problem arose in transferring and saving the images to an external source.

One week later, the second DITL test was carried out. The test was restricted to only five hours due to inclement weather, however the test was still a success. The five hours of actual tracking worked as planned and the issues from the previous test did not arise. There were no major modifications after this test and through two more systems tests, the payload was deemed ready for flight.

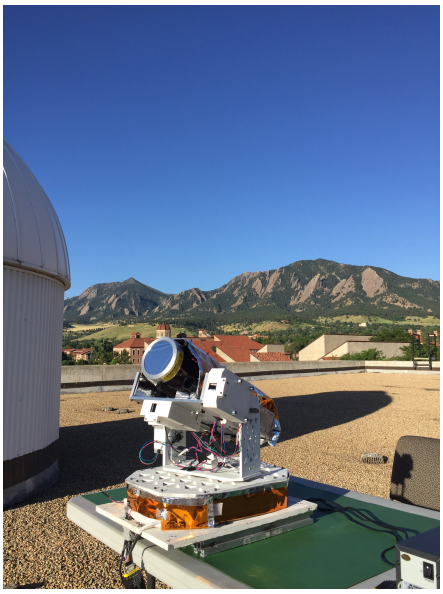

Figure 25: HELIOS tracking from roof during DITL 1

3. Ground Images for Comparison

Another purpose of the tests were to provide the set of ground images that would be compared against the flight images. This was to test if the image quality in the stratosphere was, in fact, better than the ground quality. Figure 26 is a few of the images taken during the second DITL test. As seen in these images, the Optics system was capable of capturing very clear Sun images with distinguishable sunspots.

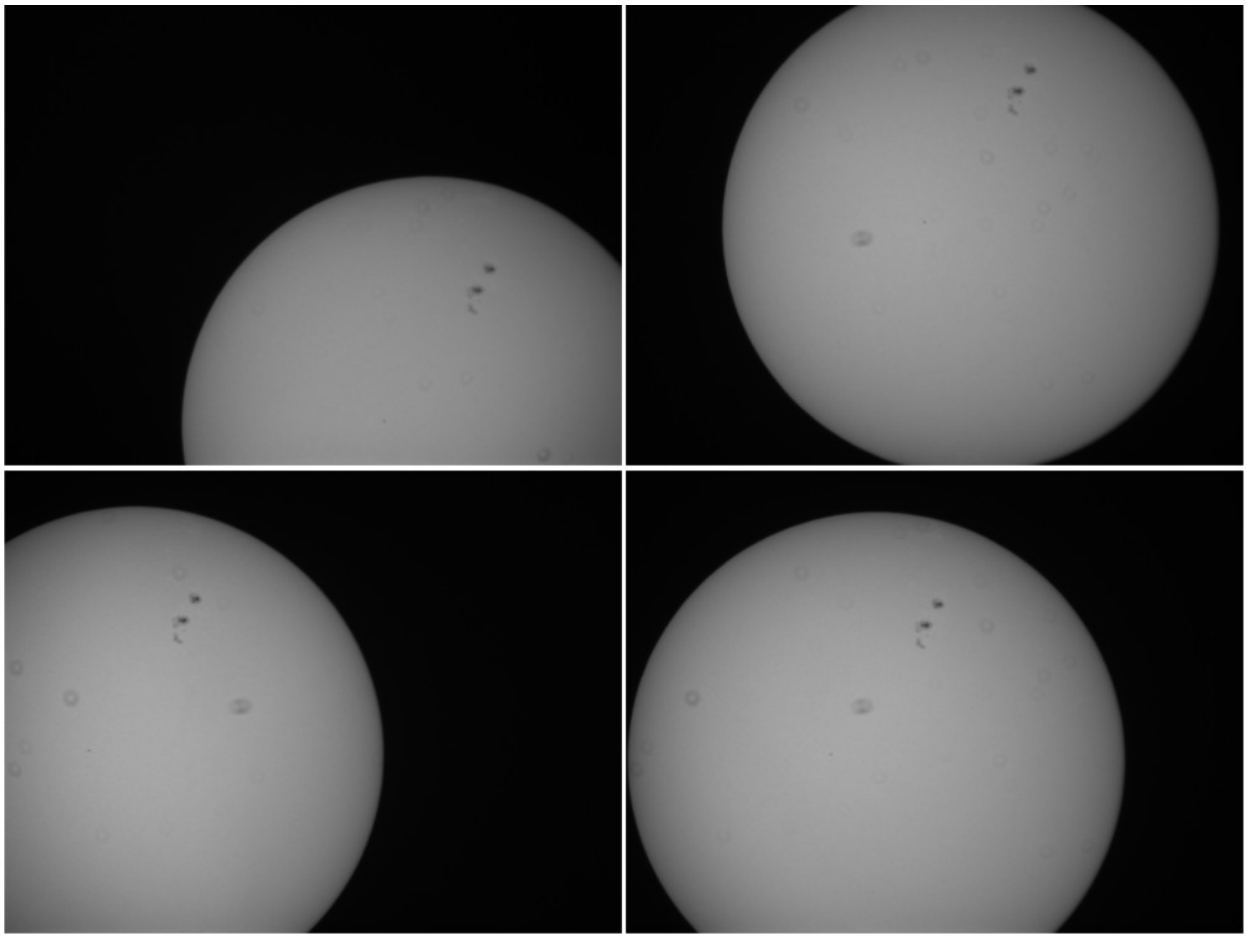

Figure 26: Sample Ground Images

E. Integration

1. Summary

During the week of July 31^{st}, five members of the team traveled to Palestine, Texas for integration at the Columbia Scientific Balloon Facility. The payload was previously tested in Boulder, however it was not tested with the actual flight gondola. The team shipped HELIOS down to the test facility in various pieces, re-integrated the telescope, and began brief tests to ensure that everything still worked. Once the payload was determined to be functional, the team hooked up the payload to HASP power and telemetry.

In addition to this, the team performed a thermal vacuum chamber test. The test began with slowly dropping the pressure to near zero, simulating the environment of 120,000 ft. Following this, the temperature was dropped to approximately -40°C and then raised again, simulating the temperature extremes that would be seen on flight. The thermal vacuum chamber was then brought back up to atmospheric pressure and the test concluded. During the test, all data was uploaded to the HASP website and the team was able to monitor the status of the payload, as well as send test commands. There were a total of two thermal vacuum tests conducted, both lasting approximately 8 hours.

The first test was conducted on August 3rd, with the payload fully integrated into the gondola. The payload worked as the pressure dropped, however once the temperature began to drop below freezing, the payload stopped functioning. No commands could be sent, the communication between the Pis ceased, and the team stopped getting data from the upper Pi. Once the temperature was raised out of the sub-freezing range, the payload began to work again, although the commands were still unable to be sent.

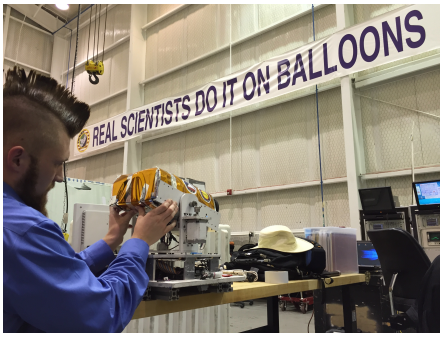

Figure 27: Finishing touches being put on new MLI protection

Due to the failure occurring at low temperatures and with the upper Pi data, it was determined that the cause of failure was the upper Pi. Following this, the team consulted a NASA engineer who worked at the facility and sought out a second opinion. The engineer gave the team freeze spray to test the Pi under similar test temperatures. However, the failure was not able to be replicated, even with temperatures below those seen in the vacuum chamber. Due to this, the team decided to change out the Pi with a back-up brought to Palestine. Furthermore, the payload did not have MLI on all sides of the upper housing, allowing for a large loss of heat. The team was able to construct a front panel with scrap MLI, as well as securing the back of the MLI in a more efficient manner, as seen in Fig. 27. With regards to the failure in commands, it was later discovered that the commands were being sent to payload 9, not HELIOS (payload 10).

After these fixes were implemented, the team conducted the second thermal vacuum test on August 5th. The payload was set-up in the exact same manner as the first test. There were no failures during the second test; the components that did not work two days before performed flawlessly. The upper housing also saw temperatures 10 degrees warmer than the first test, illustrating the improvement of the MLI protection. After this flawless test, with the combination of the other local summer tests, the team felt that the payload was ready for flight and HELIOS was shipped directly from Palestine to Fort Sumner, New Mexico, the launch location.

V. Results

A. Flight Overview

The HASP 2016 balloon launched on September 1st at 10:08 AM MST after a weather delay that morning. From this time, the flight proceeded as pictured in the timeline of Fig. 28. The major events of flight are on the bottom of the timeline in orange, while the commands sent are above in green and red.

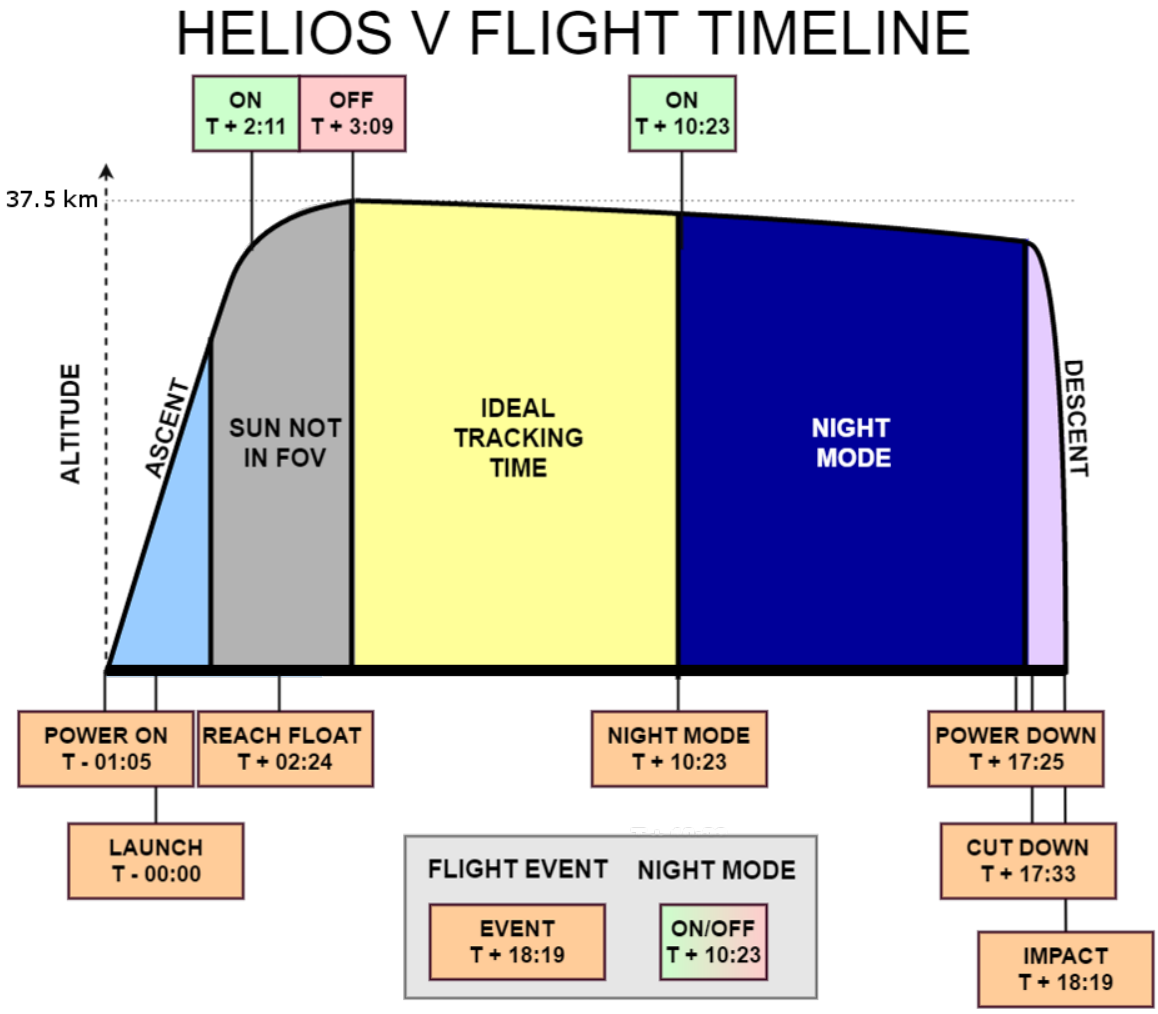

Figure 28: Flight timeline

As seen in the figure, there is a portion of ascent and float that the Sun was not in the field of view of the payload. This was due to the upper housing impacting the lower housing, restricting HELIOS V's vertical view to 60 degrees. After the Sun exceeded this limit, the team sent the command to turn on Night Mode in order to save space on the SD cards. After the Sun started to lower in the sky, the payload was able to see the Sun once again, and therefore Night Mode was turned off. The third command sent was to reactivate Night Mode after the Sun set.

The flight ended at 4:27 AM MST on September 2nd, for a total of 18 hours in flight. In this time, the payload traveled from its launch location in Fort Sumner, NM, over 580 miles until landing near Grand View, AZ. The maximum height reacted was 37.5 km.

B. Environmental Results

In addition to the science and tracking data that was collected, environmental data was also collected in order to be able to correlate the performance of HELIOS to the environmental conditions it experienced during flight; 3-axis acceleration and gyroscopic movement, pressure, and temperature. Temperature sensors placed on critical components throughout the system demonstrated that none of the components overheated.

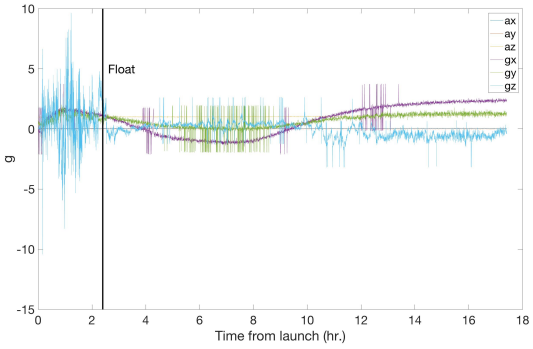

Figure 29: Acceleration and Gyroscope throughout flight

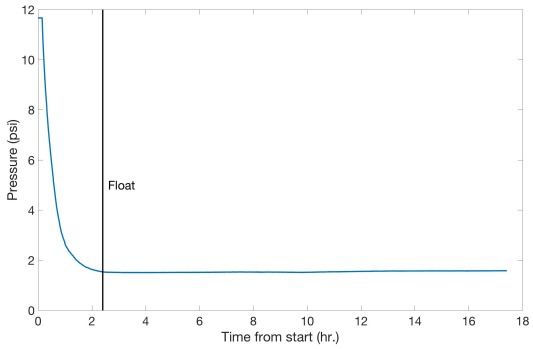

Figure 30: Pressure Throughout Flight

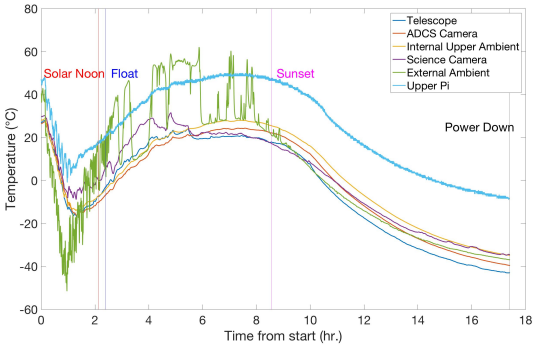

Figure 31: Upper Housing temperature

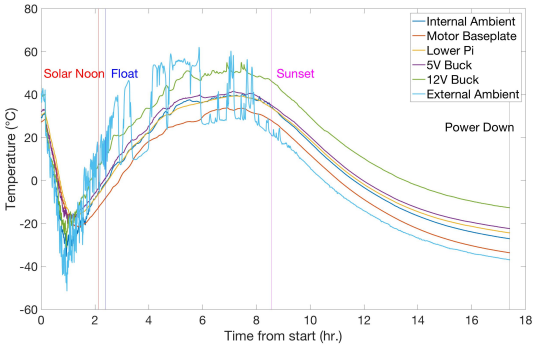

Figure 32: Lower Housing temperature

C. Subsystem Performance

1. Structures

a. Performance

The HELIOS V structure successfully supported all other systems and components throughout the duration of the flight. No components shifted out of place or broke before the system landed following the termination of the flight. This assertion can be verified by examination of the motor counts in both the elevation and azimuth directions. The counts, shown in Fig. 33 and Fig. 34 display that the tracking remained consistent across all possible ranges of rotation throughout the duration of the flight and tracking periods.

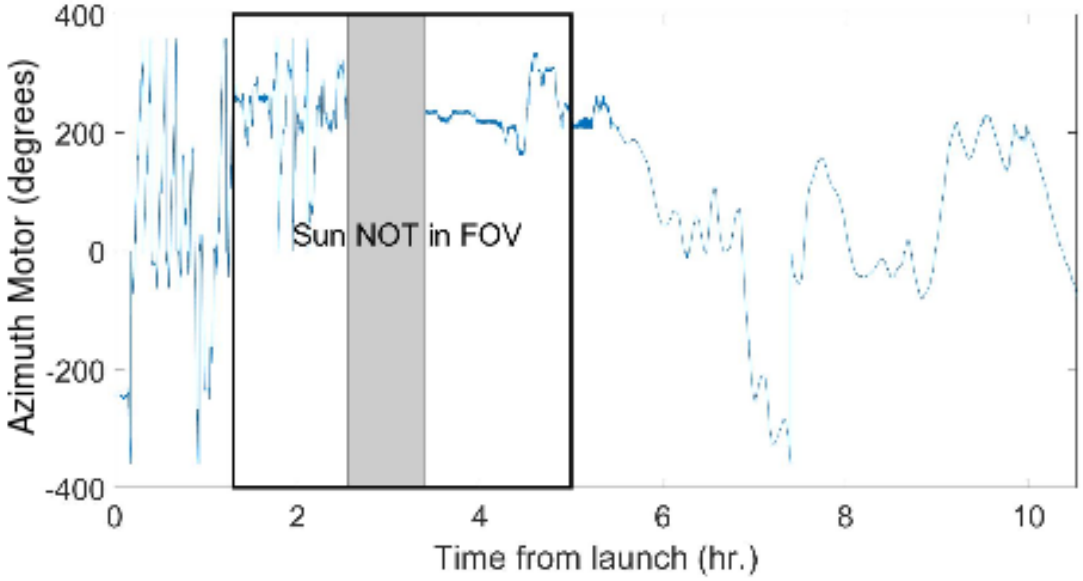

Figure 33: Azimuth Rotation Degrees Throughout Flight

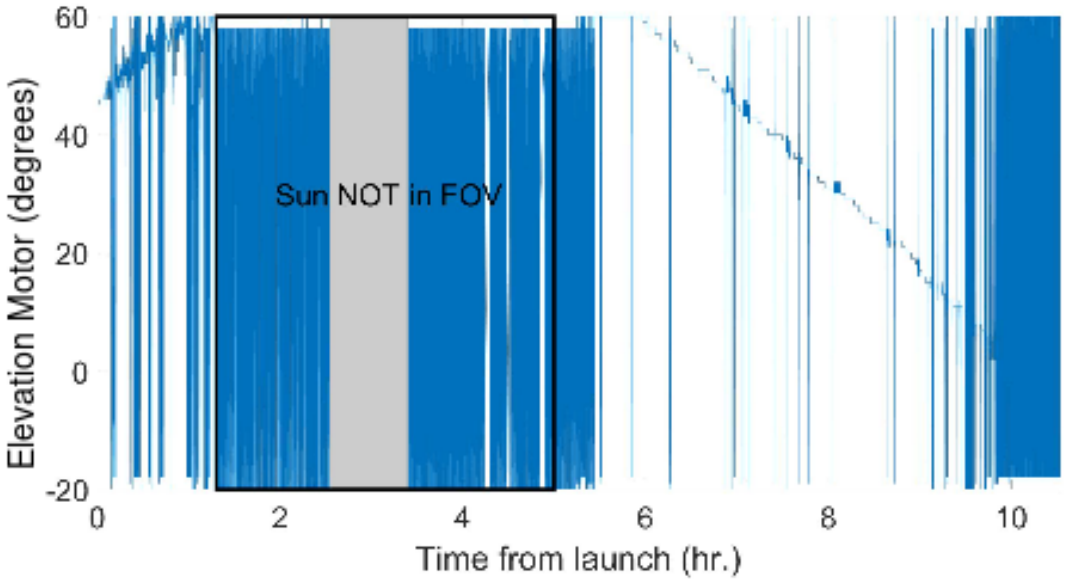

Figure 34: Elevation Motor Extension Throughout Flight

b. Flight Damages

Three structural components were visibly damaged upon recovery of HELIOS V. The L-brackets connecting the middle housing's side walls and rotary plate were both bent improperly upon landing, as shown in Fig. 35. Additionally, the bearing connecting the elevation axle was hit out of its socket upon impact on the HASP platform on the ground, as shown in Fig. 36, and the wire cover popped off of the elevation motor driver, as shown in Fig. 35.

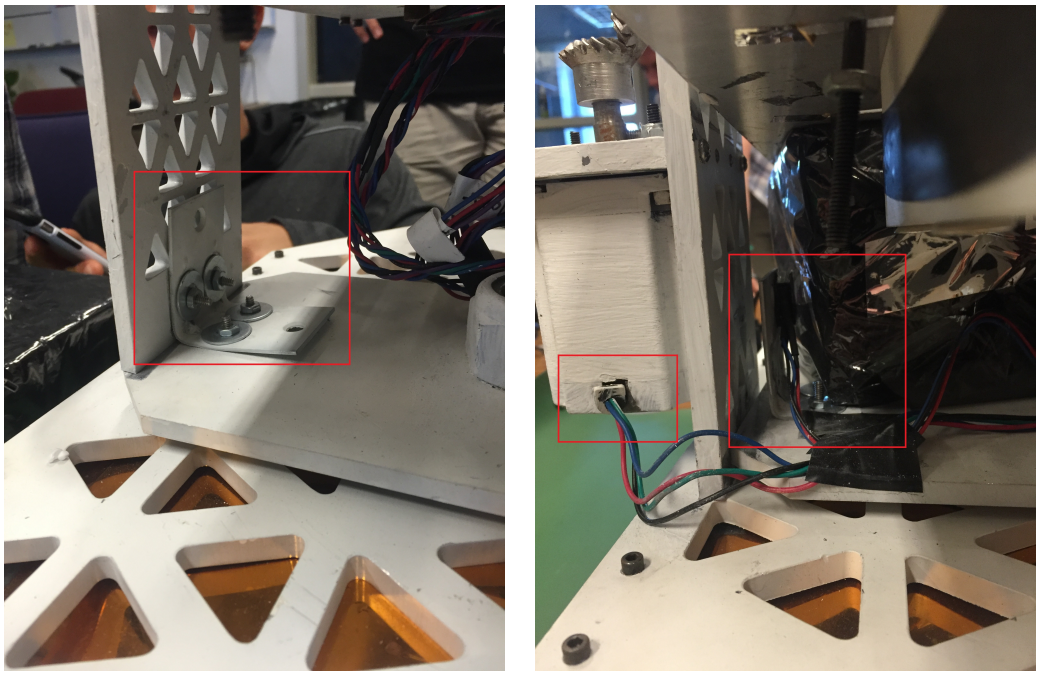

Figure 35: Bent L-bracket on Upper Housing Supports and Damaged Motor Wire Cover

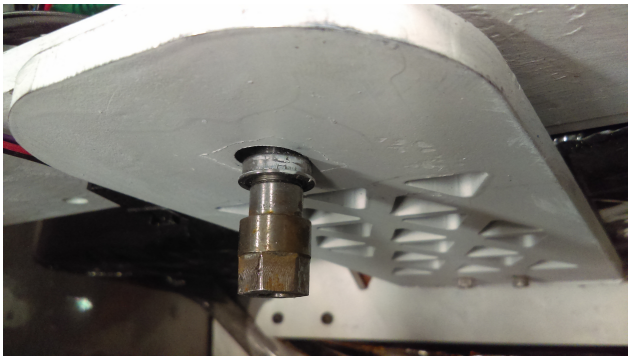

Figure 36: Bearing Knocked Out of Place

While there was no way to monitor the structure at any point after the HASP platform was cut down, all damages to the structure faced in the same direction. This can be explained by examining the orientation of the landed HASP platform as shown in Fig. 37

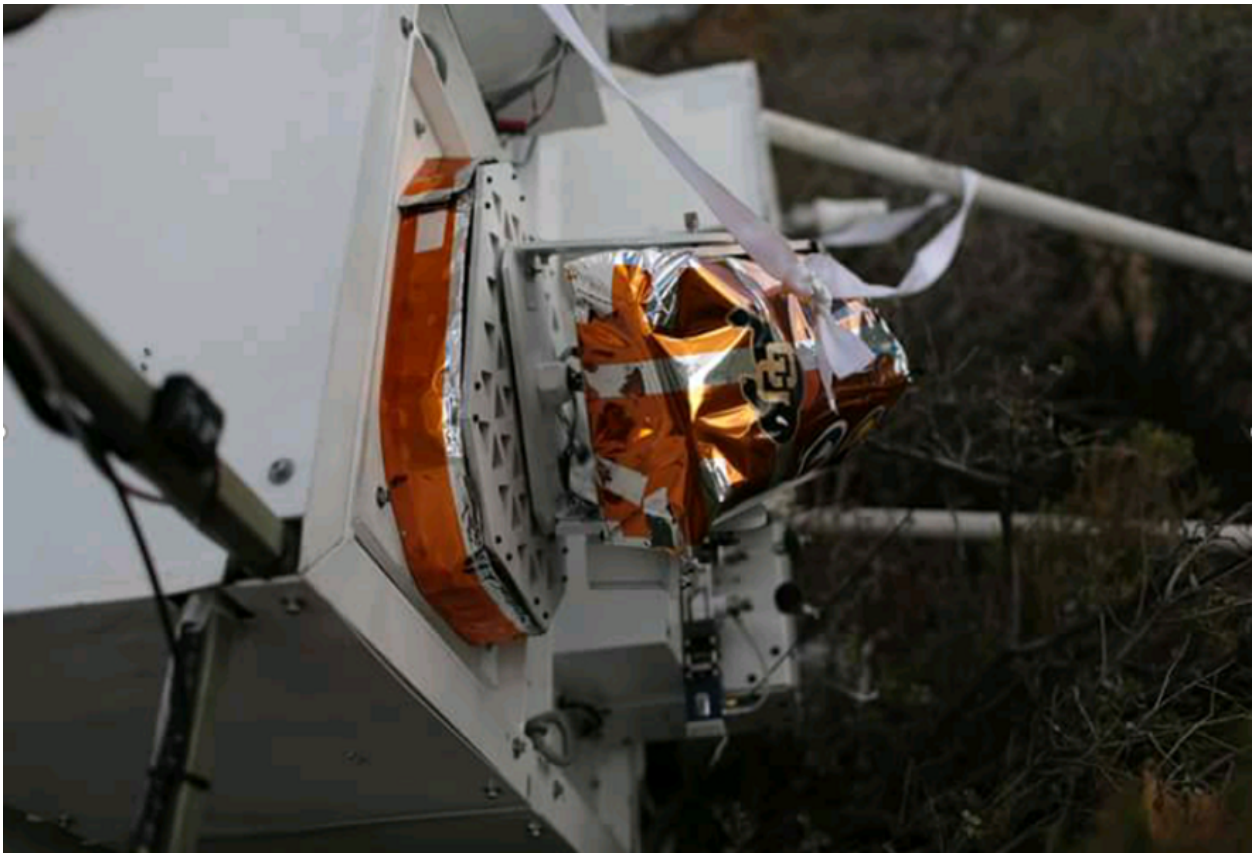

Figure 37: Landing Orientation of HELIOS on the HASP Platform

2. Optics

a. Performance

The HELIOS V optics system successfully imaged the Sun in the H-α wavelength throughout flight. However, the images were not properly focused despite the team's precautions. The cause is believed to be either an unintentional misfocusing of the telescope during testing, or a change in focus of the telescope between final flight checks and launch. This is discussed more thoroughly in the Error Analysis section found below. The HELIOS V Optics system captured 16,291 total science images during flight. Throughout the mission, all optical hardware and software operated properly.

Of the science images captured, 3,268 of them were considered successful based on the Requirements' definition, meaning they contained at least 50 percent of the Sun. The number of successful optics images as a function of flight time is shown below in Figure 38.

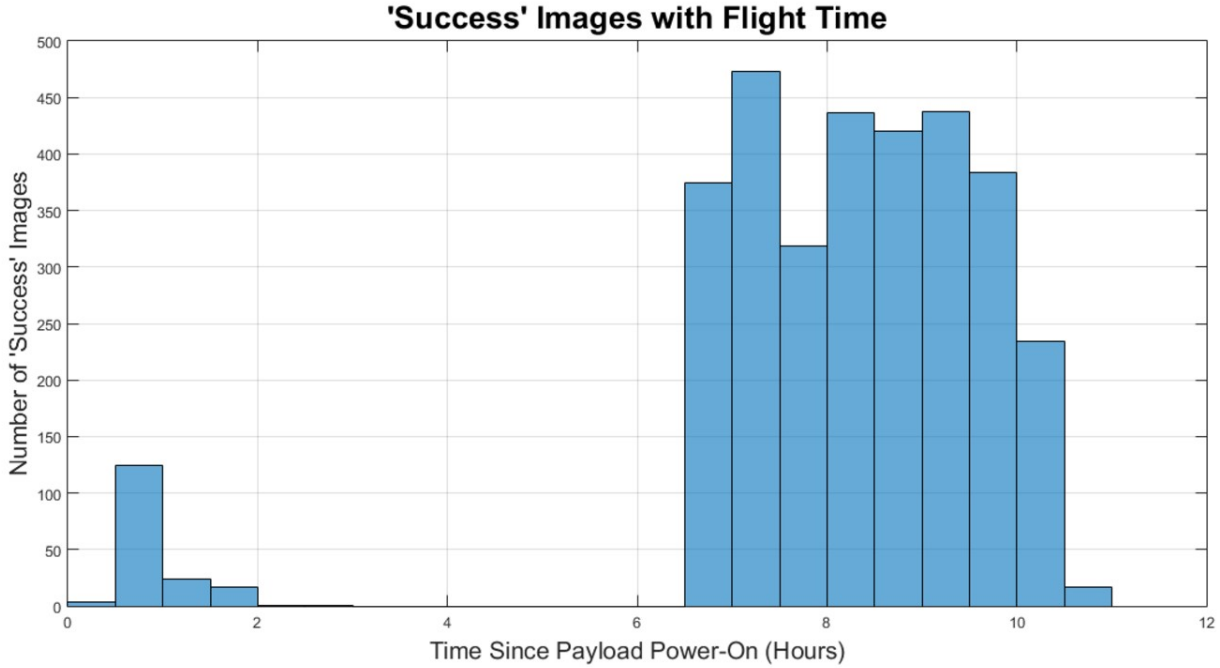

Figure 38: Optics Success Images with Flight Time

It can be clearly seen from Figure 38 that the majority of success images were taken from approximately 6.5 to 10.5 hours into flight. This predictably corresponds with the ADCS tracking data and Flight Timeline. In addition to this, it can be noted that some successful Sun images were taken during ascent. Again, no science images were taken between approximately three and six and a half hours into flight as the payload was put into night mode.

b. Flight Images

Figure 39 shows the sunspots on September 1st from NASA's Solar and Heliospheric Observatory (SOHO) satellite. From testing, the Optics team would have expected to see similar images to Fig. 39 from flight.

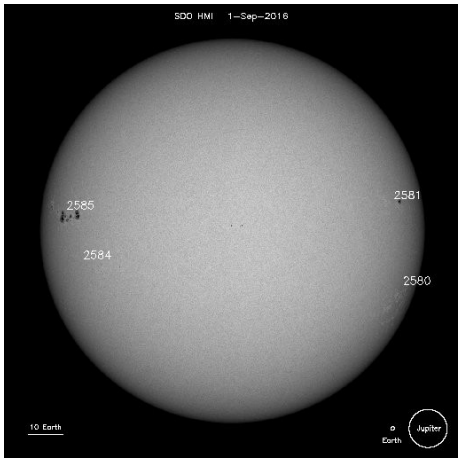

Figure 39: SOHO image from flight day

Instead, due to the focusing problems that will be further discussed in the next section, the flight images were blurred in a variety of ways. A sample of the flight images are seen in Fig. 40.

The first image shows what the best images from flight looked like. They were still blurred on the edges, and were too blurred to show sunspots. These made up the majority of the images from flight. The second and third images are examples of more badly blurred images. These images were were primarily taken in the first three hours of flight; the blur is likely caused by motion of the platform. Accelerometer data confirms this was the most unstable period during the mission. The Optics team believes that this blurring can be attributed to the motion of the gondola during flight. Motion blur can be characterized by asymmetrical smearing, which can be seen in both of the latter two images in Fig. 40. Such extreme motion blurring was never encountered during systems testing, making gondola motion the likely cause.

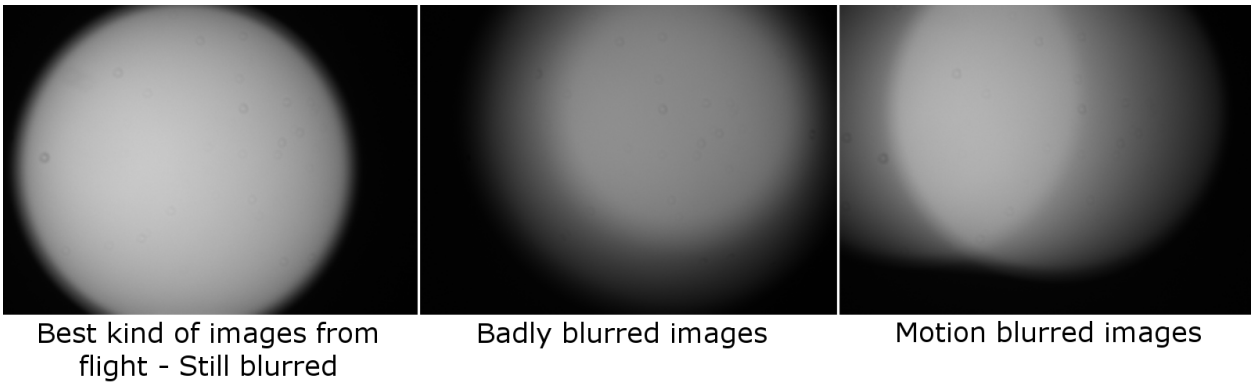

Figure 40: Sample Flight Images

c. Failure Analysis

The optics system the day of flight did not provide as sharp of images as produced previously on the ground during DITL testing. The immediate post-flight HELIOS V analysis offered several possible reasons the sub-optimal focusing:

1. Back of the telescope was not in its usual orientation when the payload was returned
2. Internal issue in the focusing of the telescope
3. Some sort of condensation over the primary Mylar filter
4. Blurred images were exclusively the result of platform slew
5. Some other sort of unaccounted factor as a function of altitude
6. Telescope was incorrectly focused in pre-flight checks
7. Focus was somehow altered or bumped between final pre-flight checks and launch

Upon further inspection of the optics system post-flight, it was immediately apparent that the telescope focus was approximately a half turn off from the correct location. While this could offer an immediate explanation to blurred images, it was not possible to conclude that the state in which the optical system was returned was the same one in which it was flown. In order to gain the most data from the optics system post-flight, it was necessary to image the Sun in the exact configuration that was returned to the team in. Unfortunately, as the full payload was unable to be repaired due to budgetary issues, all optics post-flight testing took place independently of the payload. The procedure used a simple telescope stand to image the Sun instead of the full mounting. Based on this post-flight testing it was immediately clear that images taken using the post-flight configuration were visually similar to images taken during flight, seen in Fig. 41. This was also verified from an quantitative standpoint using the same image analysis code ran on the flight images, which confirmed that the two sets of images were very similar.

Despite small flight damages to the optics system, after proper focusing of the telescope it produced successful and focused science images on par with those that were seen during DITL testing. This effectively ruled out the possibility of the unfocused images being a result of the telescope being internally damaged.

The possibility of condensation or other atmospheric effects was also considered. Though possible, if either of these were the case one could have expected to see a continuous depreciation of image quality throughout flight as the payload increased in altitude. Instead, as previously shown, image quality remained relatively the same throughout flight. In addition to this, if image blurring were the effect of some sort of condensation over the filter, this would not be a permanent effect. Instead we would see a small set of images that were heavily distorted while others appeared normally as the condensation evaporated with increasing altitude.

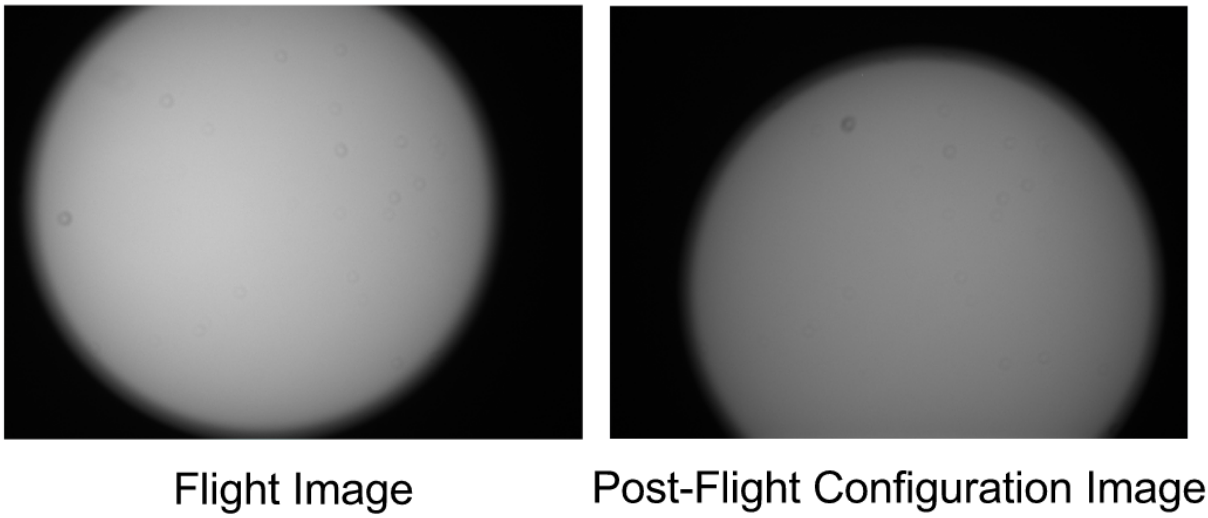

Figure 41: Comparison of flight and post flight images

The final theory of a cause for blurred flight images was that they were exclusively the result of platform slew throughout flight. If this were the case, we could expect images to be blurred almost exclusively the horizontal direction, and could expect all images to have some sort of pixel smearing. This was not the case, as the majority of science images had similar pixel slope values in the horizontal and vertical directions. This is shown in Fig. 43. In addition to this, there is a clear differentiation between what are clearly motion blurred images both visually and from a quantitative standpoint. This can be seen in the upward skew of pixel slope values from flight.

Based on all these facts, it was concluded with relative confidence that the blurred images experienced throughout flight by the HELIOS V optics team were a result of the misfocus of the telescope. Not only do images taken in the post flight configuration compare extremely well visually, they also share similar characteristics in code based analysis.

d. Computational Image Analysis

The optics team developed a Mathworks™MATLAB script to quantitatively analyze the image quality of pictures taken by HELIOS V. This script created pixel plots, as seen in Fig. 42, which were used as a measurement of how in focus an image was. To do this, the script first found which images contained at least 50 percent of the Sun, and then found where the center of the Sun was located in the images. From there, the script read in the pixels of the images as values ranging from 0 to 1, 0 for a black and 1 for white. The script then averaged the five center rows and columns around the center of the Sun to reduce the noise in the pixels, and accounted for motion blur in both the vertical and horizontal directions.

The script then found the slope of the plot during the transition in the image from the black background to the disk of the Sun (seen as a red line on the plot). This slope approached vertical as the image became more in focus, allowing the Optics team to quantitatively measure the focus of the image by finding the slope of the transition.

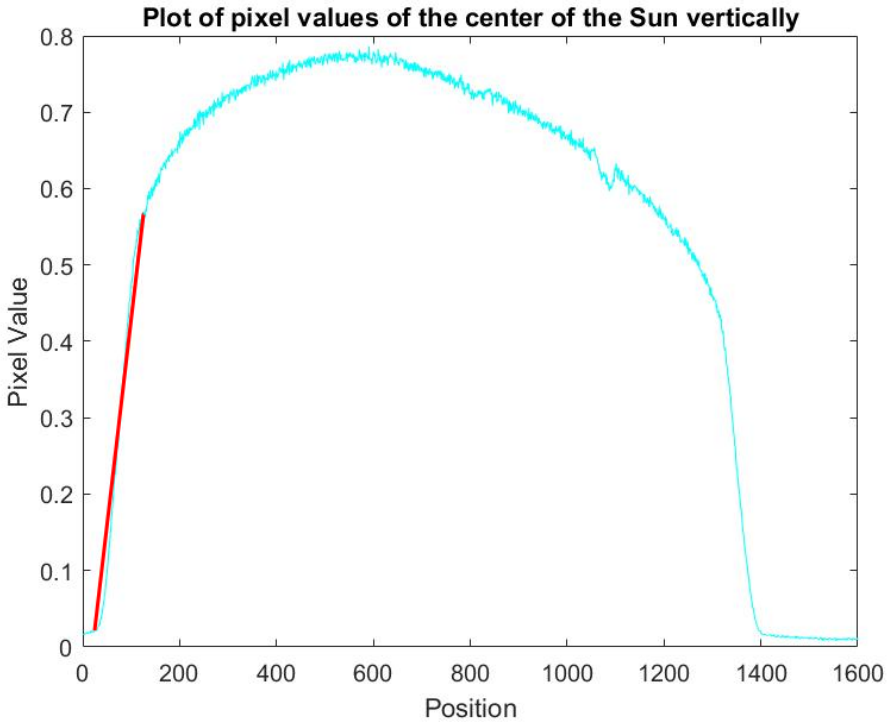

Figure 42: Sample pixel plot from a flight image

Figure 43 shows several sample images with their corresponding pixel plots. This figure includes a properly focused image from the second DITL test, as well as an image taken post flight as part of the optics failure analysis.

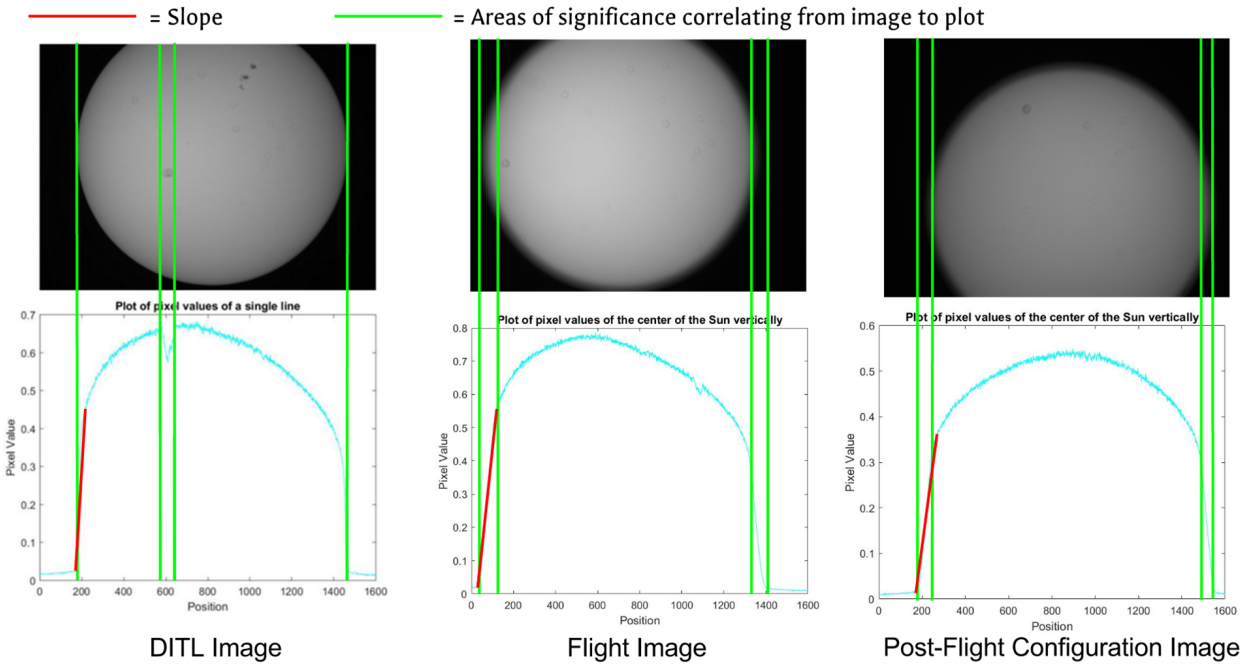

Figure 43: Comparison of Plots of DITL to Flight to Post-Flight

With the slopes found, the optics team was able to plot the slopes throughout flight to see if there was a trend. If the optics system had been properly focused, the team would have expected to see a positive trend between slope and time during the ascent portion of the flight. This is because the team expected the images to improve with altitude of the payload. The resulting plots can be seen in Fig. 44.

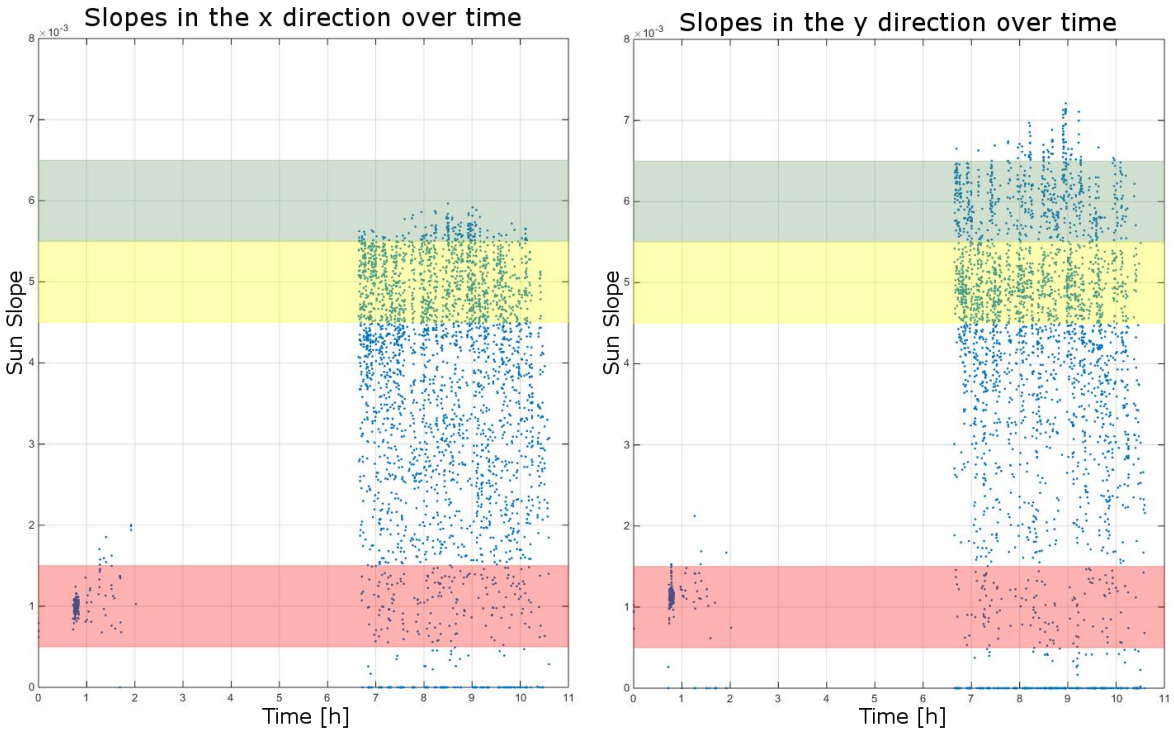

Figure 44: Focus of the images throughout flight. Green bars correspond to the best types of images with only focus blurring. Yellow images have minimal distortion by motion blur, resulting some smeared pixels. Red images tend to be extremely motion blurred, and correspond primarily to flight times in the first two hours of flight.

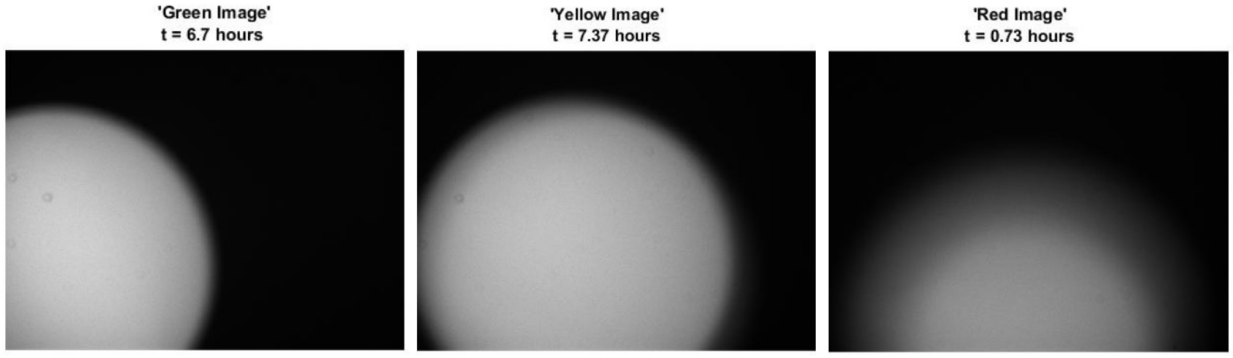

Figure 45: Distinctions of Flight Images

As noted previously, the Sun was out of the field of view for much of the ascent, so there is a gap from three to six and a half hours into flight. As seen above, there are three different highlights on the graph corresponding to three distinct types of flight images. These types or flight images are shown below in 45. Green images correspond to the best types of images that were taken throughout flight. They are sharper than yellow images which tend to be minimally distorted by motion blur resulting in smeared pixels. Finally

red images tend to be extremely motion blurred and correspond primarily to flight times in the first hour of flight. In addition to this, it it important to note that the majority of green and yellow images were taken later in flight compared to red images.

There were significantly fewer images taken during ascent, making it difficult to draw any sort of conclusive correlation between image quality and flight time. Despite this, a general trend of increasing pixel plot slope can be seen as the payload increases in altitude. Although these results are far from definitive, the hypothesis of increased image quality outside the atmosphere seems to be correct.

3. Attitude Determination and Control Systems

a. Performance

The performance of the ADCS system was exactly as the team expected, with only a small loss in tracking ability on the moving platform compared to the ground. HELIOS IV's tracking results were used as a benchmark for the tracking ability of this mission. The ADCS team was apprehensive about changing the tracking algorithm and worried about the effects on the performance of the system. The worries proved to be unfounded, as HELIOS V demonstrated a 57% increase in tracking ability compared to HELIOS IV, measured by successful image captures. The falling counterweight during the flight of HELIOS IV and the improved tracking algorithm of HELIOS V presents the most likely sources of these improvements.

The goal of the subsystem was to produce the most images within the field of view of the science camera as possible. In total, 43% of the science images taken met this criteria, and 76% were within twice the size of the field of view.

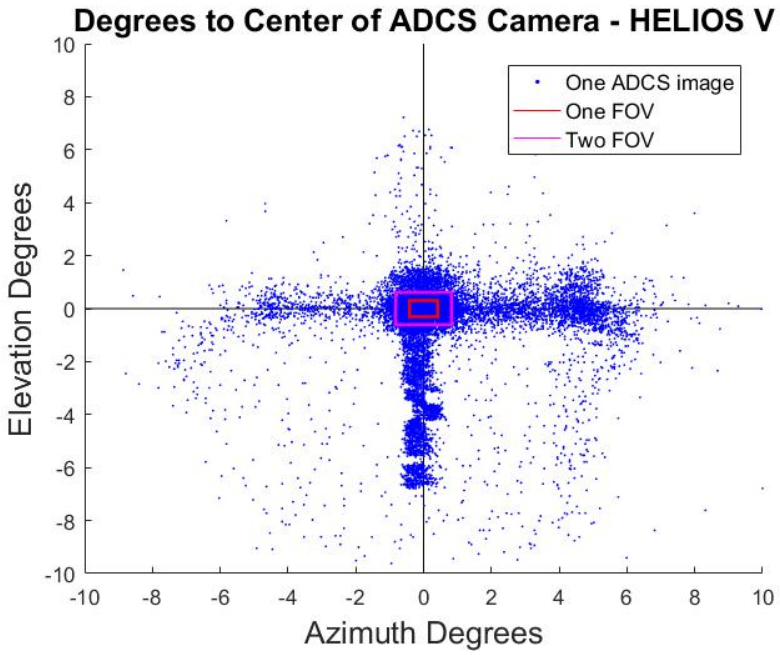

Figure 46: Scatter plot of the degrees from the center of the Sun to the center of the ADCS camera.

The "tails" off of the main group are a byproduct of the modified tracking algorithm. When the payload lost track of the Sun, it quickly panned up to the maximum, then slowly scanned down until it found the Sun. During this slow scan downwards, clumps of images spaced in roughly one degree increments were taken.

The motion and rotation of the payload were expected to cause some issues in tracking ability of the payload, so the success-images-per-minute rate was compared to both the accelerometer and gyroscope

measurements from the flight, in hopes of finding come correlation. Surprisingly, no correlation was found between the acceleration and rotation with the tracking ability. The R values for acceleration were found to be so low as to be insignificant. The tracking algorithm's main loop runs six times per second, which evidently was more than enough to combat the natural drifting of the platform.

4. Command and Data Handling

a. Performance

The CDH system performed exactly as it did during all day in the life tests. All of the threads continued their full functionality through the duration of the flight. Communication with the ground was consistent, all data was logged as expected, and the two Raspberry Pi's remained in contact.

Only three commands were sent over the duration of the flight: `Night mode ON`, `Night mode OFF`, and `Night mode ON`. All three commands performed their intended task promptly without any problems.

The usage of the Upper Raspberry Pi's Micro SD card storage linearly increased throughout the duration of flight. Disk usage reached a maximum of 65% of the 128GB storage, which verified the team's predictions of image space requirements.

The only issue from flight was that the health and status LEDs were hard to see during flight because of the Sun's glare. The LEDs were still beneficial in the testing phase of the payload, and the team believes they were a worthwhile addition despite flight difficulties.

5. Electrical and Power Systems

a. Performance

The EPS system performed nominally during flight. From periodic visual assessment of the HASP Environmental Display, there was never any significant lull or surge in the payload's voltage or current consumption. The payload maintained an average current draw of about .7 A throughout the flight, which was the current draw seen during systems and DITL testing. While safe mode was activated, the voltage and current dropped because the camera system was disabled. This was expected as the camera system had the largest power requirement.

All components remained on during the entire duration of flight, indicated by the continuous stream of downlinked telemetry from all sensors, the Raspberry Pi, the motors, and the ADCS camera. The number of pictures taken by the the ADCS camera and the science camera match the expected numbers based on the rate established in systems testing.

b. Heat Sink Requirements

From previous HELIOS missions and testing, it was determined that the motor drivers which control the motor movement generate a significant amount of heat. Because these components were directly attached to the EPS board, it was necessary to draw the generated heat away from the board to protect the circuitry. One end of copper braid was attached to each driver, and the other end was attached to the base plate with a thermal compound. As seen in 47, the azimuth and elevation base plate reached a maximum temperature of 57°C and 44°C , respectively. The copper heat sinks effectively reduced the heat of each by around 10°C, keeping the azimuth and elevation drivers at a safe temperature of 39°C and 36°C, respectively.

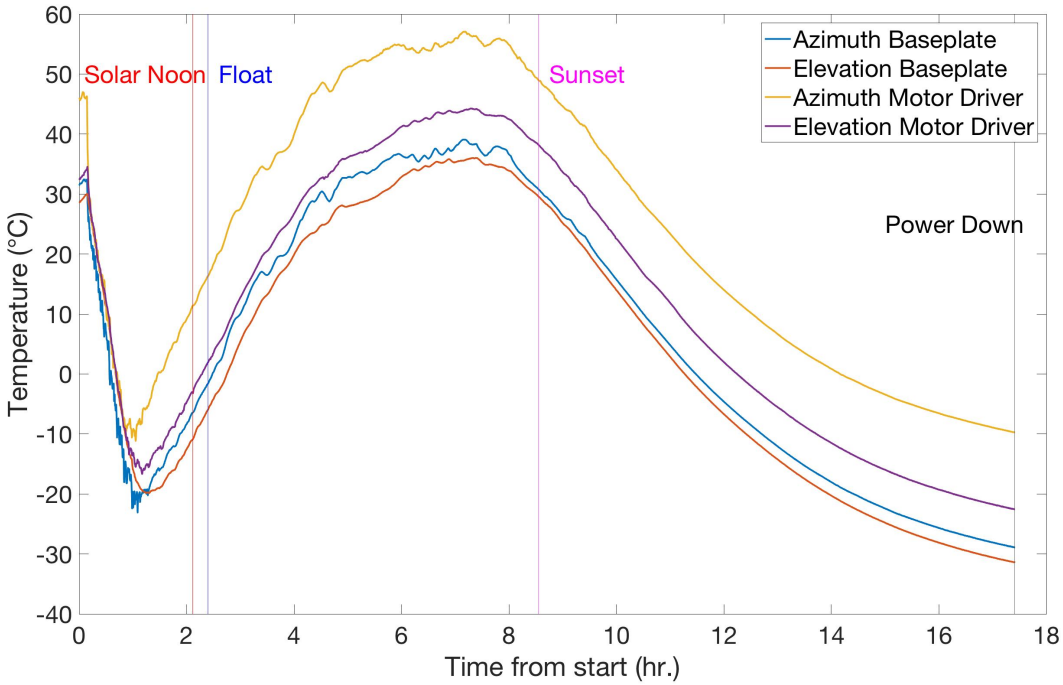

Figure 47: Graphical illustration of successful heatsink

c. EPS Post-Flight

Following flight, all EPS components were assessed for damages. Nearly all wires, including those connecting cameras, boards, and connectors were intact and undamaged. The exception was the wires connected to the elevation motor, as seen in Fig. 35. These likely dislodged during the hard landing, and did not affect motor performance.

Following the damage check, the payload was turned on to ensure that it was still in running order. However, the payload was sending current back into the power supply. The initial assumption was that a short occurred on the EPS board, rendering it irreparable. The team was able to rebuild the power connector and the problem persisted, supporting the initial assumption.

D. Alignment Results

To determine the accuracy of camera alignment, the number of successful pictures taken by both the science camera and tracking camera were compared over spans of 30 minutes. As seen in Fig. 48, there is a positive correlation between the number of successful tracking images and successful science images. The two variables are correlated with an R value of .99 and a P value of .97, indicating that 97% of the successful images were taken when the the Sun was science camera was centered on the Sun. This shows that the science camera and ADCS camera were correctly aligned. This is significant because any instrument that requires tracking of the Sun could be put in the position of the telescope using the alignment procedure and guarantee that the Sun would be in the view of the instrument about 97% of the time.

E. HELIOS V Compared to HELIOS IV

The scatter plots in Fig. 49 show the center of the Sun compared to the FOV of the science camera, as captured by the ADCS camera. 43% of the tracking images taken by HELIOS V were within the FOV of the science camera. A similar plot was constructed for the data from HELIOS IV using the same success

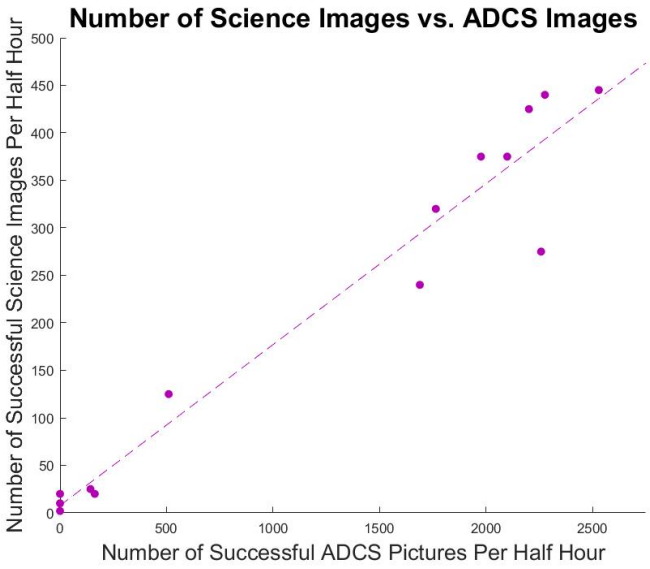

Figure 48: Positive relationship between number of successful ADCS images to successful science images.

criteria. HELIOS V on average had 47 "successful" iterations of the tracking loop per minute, while HELIOS IV averaged 25, showing an increase of 88%. This signifies that after the HELIOS V team was able to repair the damages that occurred on HELIOS IV, the HELIOS V team was able to prove the success of the tracking system developed for HELIOS IV.

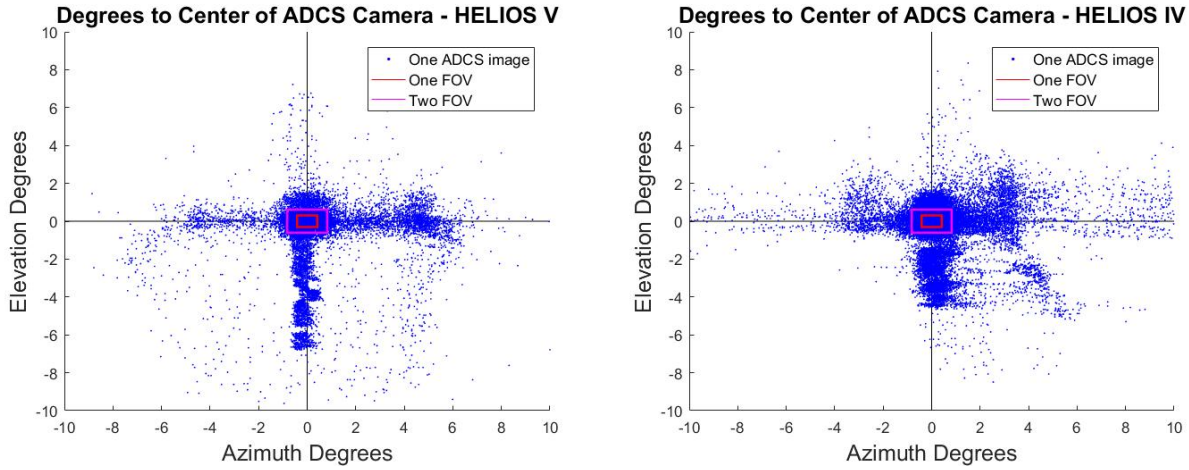

Figure 49: Comparison of density of Sun center in tracking images

The heat maps in Fig. 50 show the density of the location of the center of the Sun in all of the tracking images. Compared to HELIOS IV, HELIOS V had a greater density of Sun centers in the successful range, which is again shown in terms of FOV of the science camera. While the low density for HELIOS IV is due to the fallen counterweight, the results from HELIOS V show that without the failure mode of the fallen counterweight, the tracking system from HELIOS IV could have tracked the Sun equally well. Both HELIOS V and HELIOS IV show a tendency to track towards the bottom of the FOV of the science camera. For future missions, this could be corrected by changing the elevation bias on the ADCS camera so that it centers itself at a steeper angle.

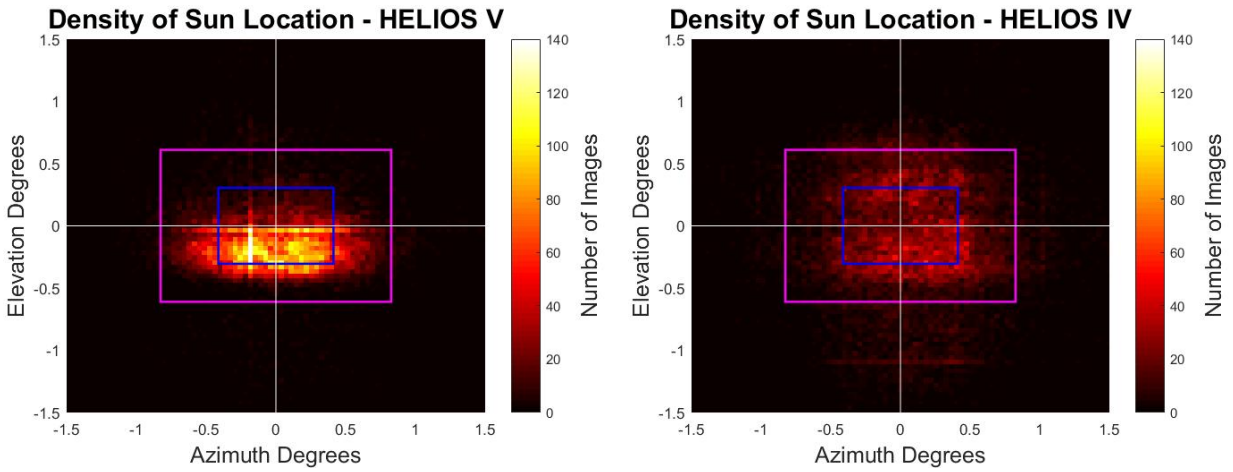

Figure 50: Comparison of density of Sun center in tracking images

VI. Mission Conclusions

A. Mission Objective

Mission Statement: HELIOS V will use the HELIOS IV tracking system to track and take pictures of the Sun in the Hydrogen Alpha wavelength.

The HELIOS V team was successful in its use of the tracking system of HELIOS IV, with only minor changes to be addressed in Subsection C. The system successfully tracked the Sun throughout flight, as seen in the graphs and live video of the payload. The payload also took approximately 14,000 images of the Sun with a Hydrogen-Alpha filter, allowing the team to see through the upper layers of the Sun. Although the telescope was out of focus, it is likely that the system would have captured the solar features during flight, as supported by testing images.

B. Minimum Success Criteria

1. **Show better image quality on HELIOS vs. ground**

   Based on initial observations of the data, the payload was unable to take images with better quality during flight than on the ground. The most sharp images were taken during systems and DITL testing. However, the image focus over time data, seen in Fig. 45, displays a upward trend of image quality. This is not conclusive due to the lower quality images occurring during ascent as well as the lack of images from the two to six and a half hour mark.

2. **Average 5 successful (focused, 50% of Sun) science pictures per minute during solar tracking time** Unfortunately, the team was unable to have in-focus images, thus rendering this success criteria a failure. This should not have been the case had the criteria been written in a proper manner (see section VII). That being said, the team captured approximately 8.7 science images per minute. These images have 50% of the Sun in them and had the science camera been in focus, this success criteria would have been greatly exceeded.

C. Requirements

The HELIOS V team was able to meet the vast majority of requirements set forth for the design. All of the upper level requirements were met, guiding the team in the proper direction and allowing for successful

tracking. However, there were two lower level requirements that were not met. Requirements 0.1.3 and its sub-requirement 0.1.3.1 deemed that the camera housing shall accommodate the HELIOS IV photodiode housing, and any changes to the upper housing shall not interfere with the HELIOS IV diodes. These requirements were to guide the team to *only* add an optics system to the successful HELIOS IV tracking system. However, during the testing phase, problems with the HELIOS IV elevation diodes arose and they needed to be scrapped from the mission. Had the elevation diodes been kept, the payload would have been unable to track the Sun and the mission would have been unsuccessful. In the future, the requirements should be drawn up in a manner such that they would not have to be broken to ensure mission success.

D. Overall System Functionality

All components of the payload, with the exception of the telescope focus, performed in the expected manner. Although the science mission was not a complete success, the general trend of increased image quality outside the atmosphere could still be seen in the data. The engineering mission of tracking the Sun was a perfect success, performing even better than the HELIOS IV mission. In addition to this, all of the subsystems integrated properly and performed flawlessly during flight. The Raspberry Pis communicated with each other and the HASP platform throughout flight. The tracking algorithms smoothly controlled the motors and upper housing such that the Sun was within view of the science camera when possible. With a single adjustment to the telescope focus, the system would be ready to fly again with a higher chance of success.

VII. Lessons Learned

A. Structures

1. Possible Design Improvements

The current structure was built off of the structures of the past missions, most notably HELIOS IV. There are a few design improvements that could have made it more successful. The motor shaft is a complex design that caused multiple assembly issues. It should be redesigned and re-machined for any future ventures of this structure. The photodiode housing attachment method also caused assembly issues due to the inability to access the attachment screws within them. They are also very fragile. If any future missions utilize photodiode housings, a single combined photodiode housing design would allow for ease of mounting and accessibility.

2. Weight Limitations

As with any project, the structure is limited by its weight. Originally, weight was not a concern until new parts, filters, and wires were added to the structure. It is extremely important to realize that weight will always be an issue and to keep that in mind when new instruments are introduced. The lightening cuts made to the lower and middle housing were extremely crucial in keeping the structure underneath the weight limitations. If any future instruments are added, the team will need to take into consideration the weight of the structure.

B. Optics

1. Alternative Design Approaches

The most obvious design improvement for HELIOS V's optics system would be the implementation of a locking focus mechanism. This would allow for the focus of the telescope to be set at some early point in the testing phase and no further changes would be necessary. Another option would be the implementation of a auto-focusing mechanism on the telescope. While this would significantly complicate the current method for focusing the telescope, it would effectively eliminate any sources of human error.

Another major design approach that could be changed would be the implementation of a more narrow band pass H-α filter. The implementation of a sub-nanometer filter would have a significant improvement on the quality of science images. These filters are usually costly, as well as powered, therefore putting it outside the capabilities of this mission. While both cost and hardware configurations would be significant hurdles to overcome, the improvement in what solar features could be distinguished given the current optical system would be immense. This would not only make it much easier to compare image quality from the float to the ground but could also offer more sophisticated and professional science images.

2. Alternative Analysis approaches

While the HELIOS V optics image analysis software was practical and effective, it was not as sophisticated as typical industry image analysis practices. Given the chance, the optics team would have dedicated more time into learning and implementing these techniques to the current image analysis processes.

C. Attitude Determination and Control Systems

The key takeaway for the ADCS team was that duplicates of all vital components should be considered critical. The tracking algorithm had to be modified late in the development of the payload due to electrical issues in fabricating another photodiode board, which could have caused a mission failure.

The ADCS team wishes that readings from the sensors were saved more often. More data points would allow the team to be more certain in its convictions about the effects of acceleration and rotation on the payload's tracking ability.

D. Command and Data Handling

A more robust method for verifying the health and status of the payload during flight may be needed, since the LEDs proved ineffective during flight. Backups of both hardware and software proved to be critical. During testing in Palestine, Texas, a backup Raspberry Pi had to be used due to temperature failure of the Upper Pi. Following one of the DITL tests, the science images were accidentally deleted due to the SD card filling up. After this, the CDH team adopted a policy of backing up everything immediately.

E. Electrical and Power Systems

It is necessary to document all revisions of power schematics so that further revisions can be as accurately as possible. Simply saving schematics is not enough; documentation of critical design choices can be extremely beneficial to future teams. It is important to document every electrical connection and wire on the system so that the system can be effectively powered and debugged by anyone who did not design the original power system.

Ease of access is critical, especially for testing, so it is necessary to be aware of the location of important components.

When it comes to re-using components, there are two sides to the issue. If a component is proven to have worked, tests should be carried out to ensure functionality. Through the failure of the photodiodes, it was learned that the functions and interfaces should be completely researched and understood for components from previous years that are reused.

F. Systems

Its important to know when to switch from an engineer mentality to a manager mentality. Systems engineers are responsible for questioning the team's decision making. Each subsystem has their own requirements and perspectives, but it is the role of the systems engineers to ensure that the decision is for the benefit of the mission and will achieve the objectives.

Plan far in advance for testing; it will take longer than expected to get everything properly integrated. It is easy to get off of schedule during testing, so plan for large margins.

When it comes to writing requirements, there should be no requirements that may need to be broken in order to achieve mission success. Before the success criteria are defined, understand the full limitations of the system in order to make a reasonable judgment about the capabilities of the system. Mission success criteria should not depend on each other; it should not be necessary to satisfy one criterion in order to satisfy another. Any criterion that must be satisfied prior to satisfying another criterion should be a requirement rather than a measure of success.

VIII. Moving Forward

The Colorado Space Grant Consortium at the University of Colorado at Boulder shall be submitting a proposal for HASP 2017. Due to the success of the HELIOS V mission in all aspects except focusing, COSGC has determined that there is not enough of a learning opportunity for students to consider a HELIOS VI mission. Instead, COSGC has already put together a group of students, primarily freshman finishing the Gateway to Space course, to write the new proposal. The new mission shall focus on reusable expandable habits for use in space exploration. COSGC looks forward to continuing their partnership with the HASP program and would like to thank HASP for continuing to offer such an amazing opportunity for the students at the University of Colorado at Boulder.

IX. Acknowledgments

The team would like to thank the mentors who helped with the HELIOS V mission, including Jason Glenn, Lee Sutherland, and Fabio Mezzalira, Chris Koehler, and Brian Sanders.

They also would like to thank their sponsors; the Colorado Space Grant Consortium, the Engineering Excellence Fund, and the Undergraduate Research Opportunity Program.

Appendices

A. CDH Uplink Commands

Payload command	Hex command	Description
Ping lower Pi	0xAA 0xAA	Pings payload to test communication
Toggle diode pair	0xBB 0xA0	Toggles between the main and backup set of diodes
Azimuth nudges	0xC0 0x00-0xB4	Counter-Clockwise Nudge
	0xC1 0x00-0xB4	Clockwise Nudge
Elevation nudges	0xD0 0x00-0x41	Nudge Up
	0xD1 0x00-0x41	Nudge Down
Reset motor count	0xBB 0xBF	Pan payload to hit switch to restart elevation count
Pan mode ON	0xBB 0xFA	Toggles panning mode for total diode failure
Pan mode OFF	0xBB 0xFB	
Query Safe Mode	0xAA 0xA0	Check whether safe mode is on (00 is OFF, 01 is ON)
Safe mode ON	0xBB 0xD1	Inhibits motion, leaves motors on
Safe mode OFF	0xBB 0xD0	(To be used at night to keep the system idle)
Reboot upper Pi	0xFF 0x01	Reboots upper Pi
Reboot both upper and lower Pi	0xFF 0x08	Reboots both Pi's
Turn on image analysis	0xBB 0xB1	Turn image analysis on
Turn off image analysis	0xBB 0xB0	Turn image analysis off
Faster image capture rate	0xFF 0x06	Take pictures every 2 seconds (default)
Slower image capture rate	0xFF 0x07	Take pictures every 5 seconds
Picture Status	0xFF 0x09	Displays flight time and pictures taken

10°: 0x0A 30°: 0x1E 45°: 0x2D 60°: 0x3C 90°: 0x5A 180°: 0xB4

B. PCB Schematics and Design

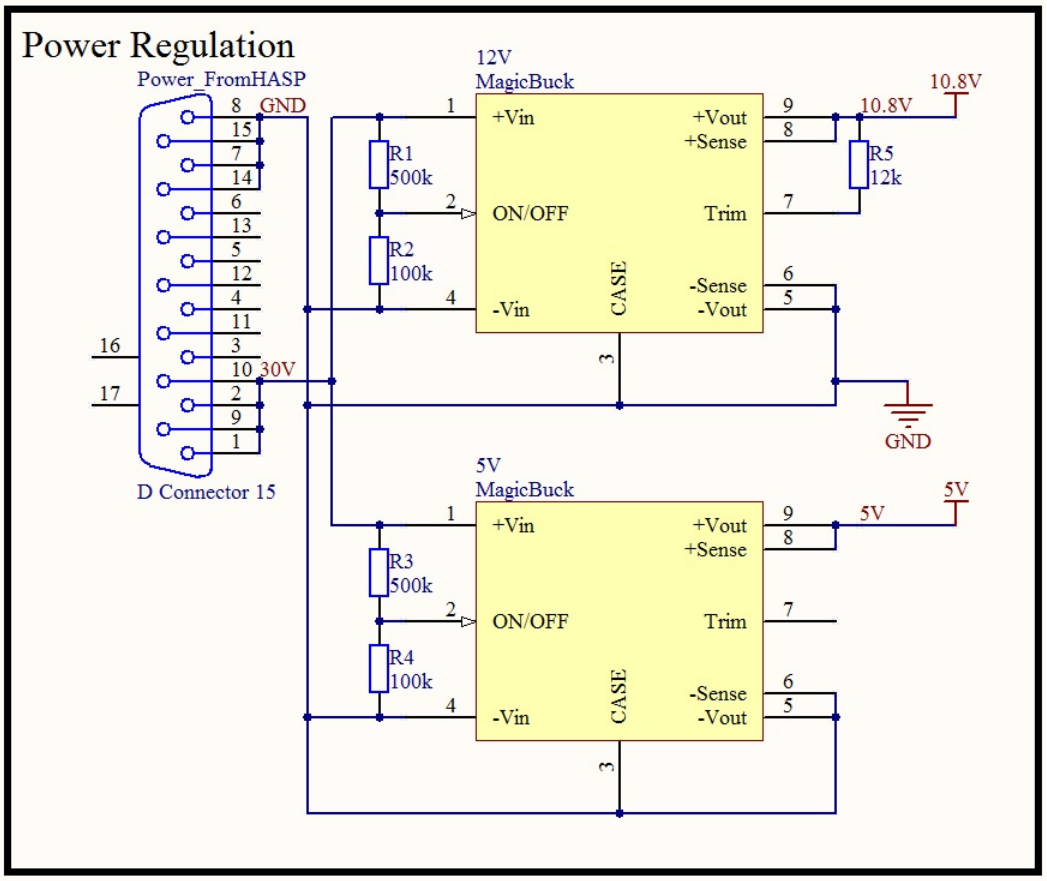

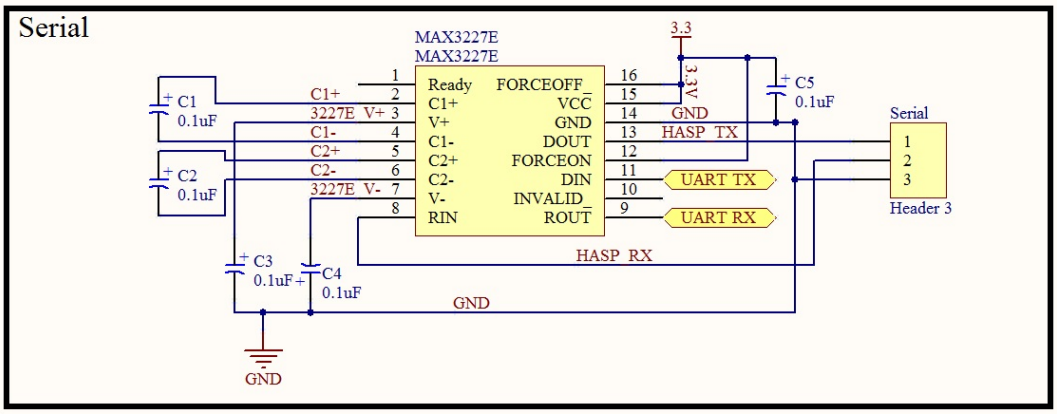

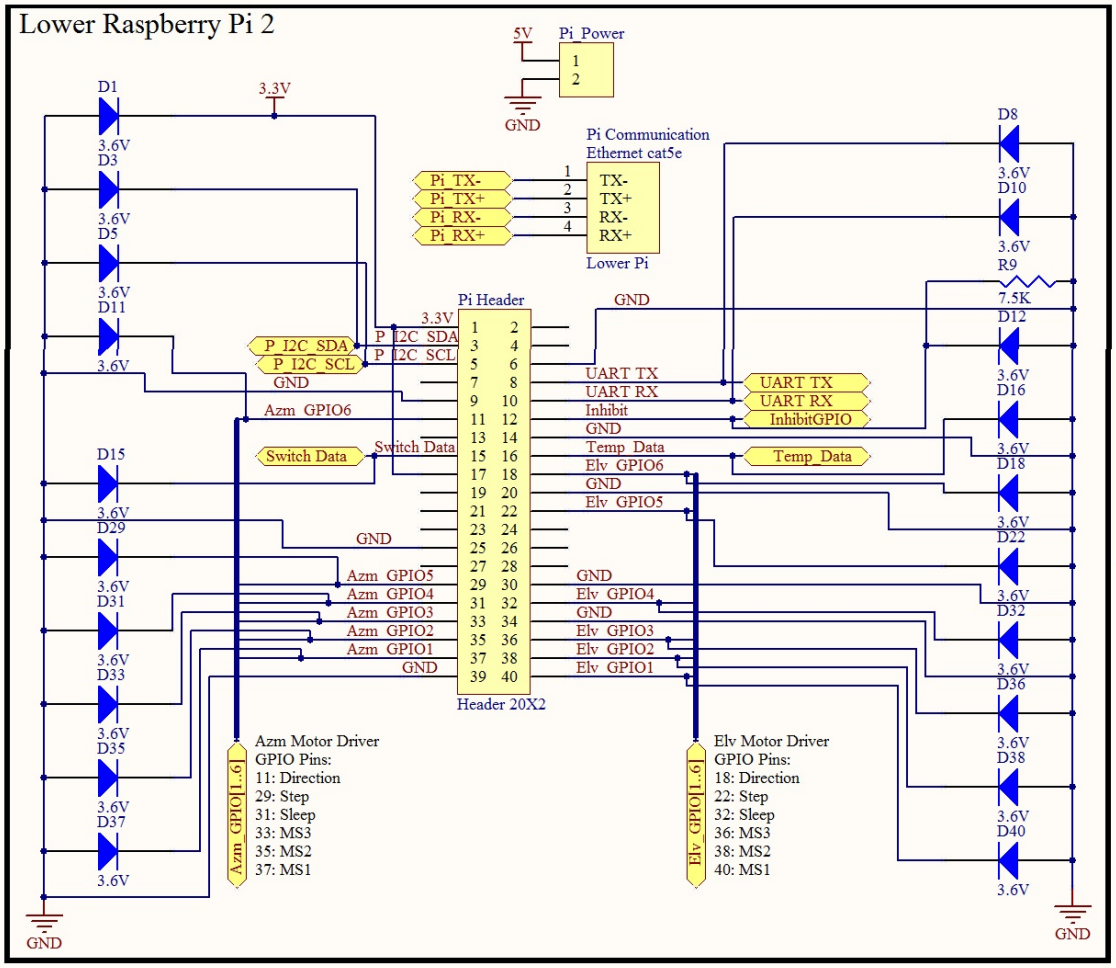
Lower Raspberry Pi 2
5V
Pi_Power
GND
Pi Communication
Ethernet cat5e
Pi_TX-
Pi_TX+
Pi_RX-
Pi_RX+
TX-
TX+
RX-
RX+
Lower Pi
Pi Header
3.3V
P_I2C_SDA
P_I2C_SCL
GND
Azm_GPIO6
Switch Data
Azm_GPIO5
Azm_GPIO4
Azm_GPIO3
Azm_GPIO2
Azm_GPIO1
UART TX
UART RX
Inhibit
Temp_Data
Elv_GPIO6
Elv_GPIO5
Elv_GPIO4
Elv_GPIO3
Elv_GPIO2
Elv_GPIO1
Header 20X2
UART TX
UART RX
InhibitGPIO
Temp_Data
D1
D3
D5
D11
D15
D29
D31
D33
D35
D37
D8
D10
D12
D16
D18
D22
D32
D36
D38
D40
3.6V
R9
7.5K
Azm Motor Driver
GPIO Pins:
11: Direction
29: Step
31: Sleep
33: MS3
35: MS2
37: MS1
Azm_GPIO[1..6]
Elv Motor Driver
GPIO Pins:
18: Direction
22: Step
32: Sleep
36: MS3
38: MS2
40: MS1
Elv_GPIO[1..6]

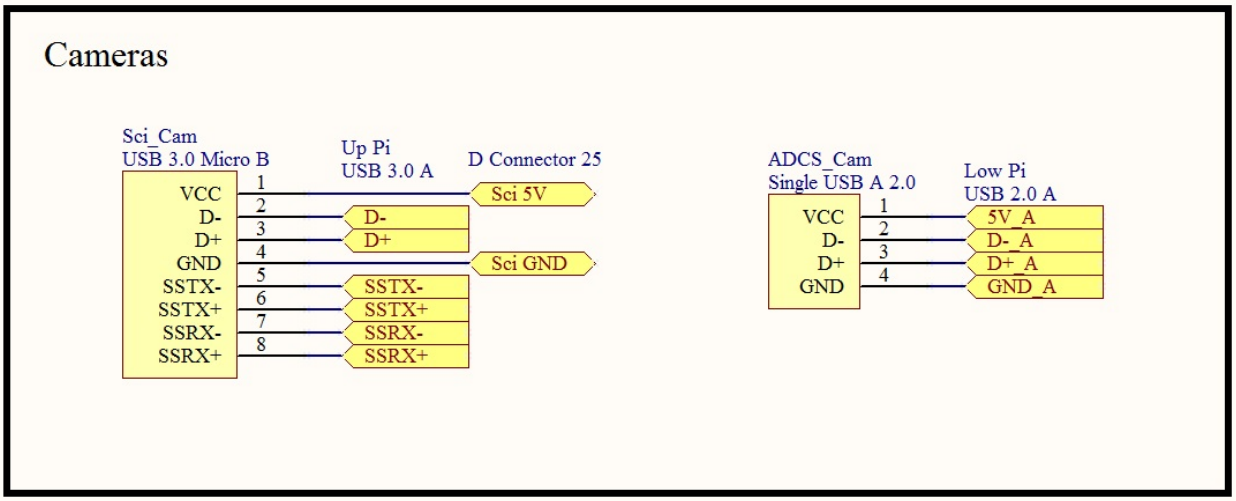
Cameras
Sci_Cam
USB 3.0 Micro B
VCC
D-
D+
GND
SSTX-
SSTX+
SSRX-
SSRX+
Up Pi
USB 3.0 A
D Connector 25
Sci 5V
Sci GND
ADCS_Cam
Single USB A 2.0
Low Pi
USB 2.0 A
5V_A
D-_A
D+_A
GND_A

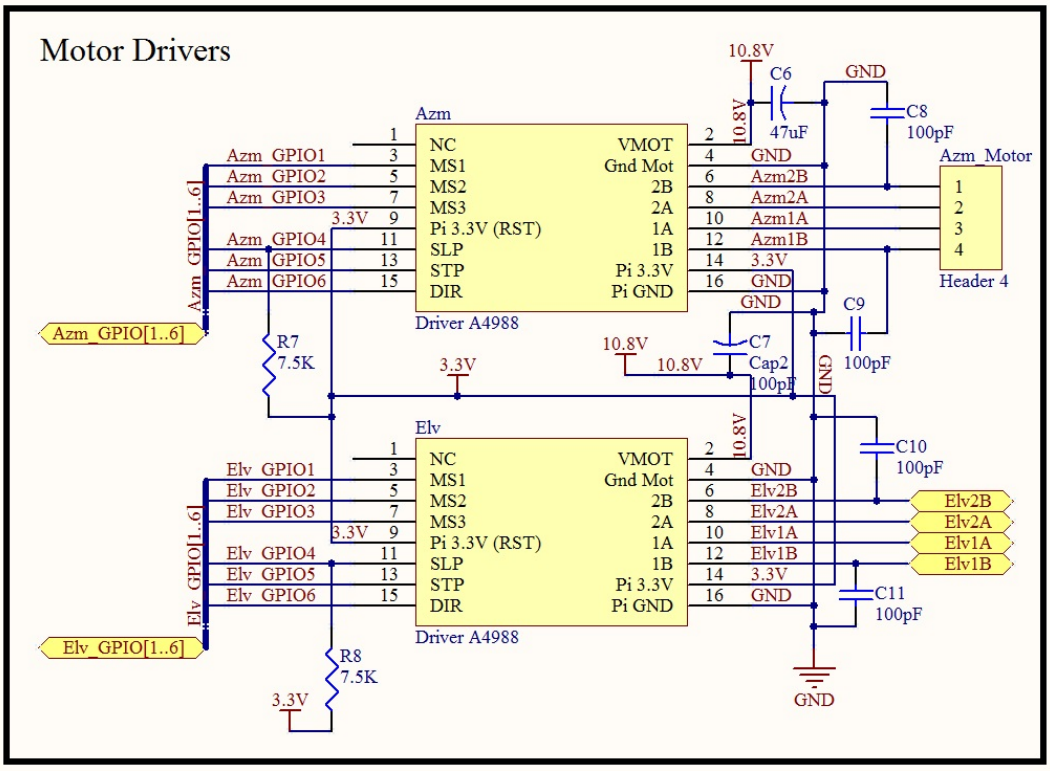
Motor Drivers
Azm
Elv
NC
MS1
MS2
MS3
Pi 3.3V (RST)
SLP
STP
DIR
VMOT
Gnd Mot
2B
2A
1A
1B
Pi 3.3V
Pi GND
Driver A4988
Azm_GPIO[1..6]
Elv_GPIO[1..6]
Azm_Motor
Header 4
Elv2B
Elv2A
Elv1A
Elv1B
10.8V
3.3V
GND
C6
47uF
C7
Cap2
100pF
C8
C9
C10
C11
R7
7.5K
R8

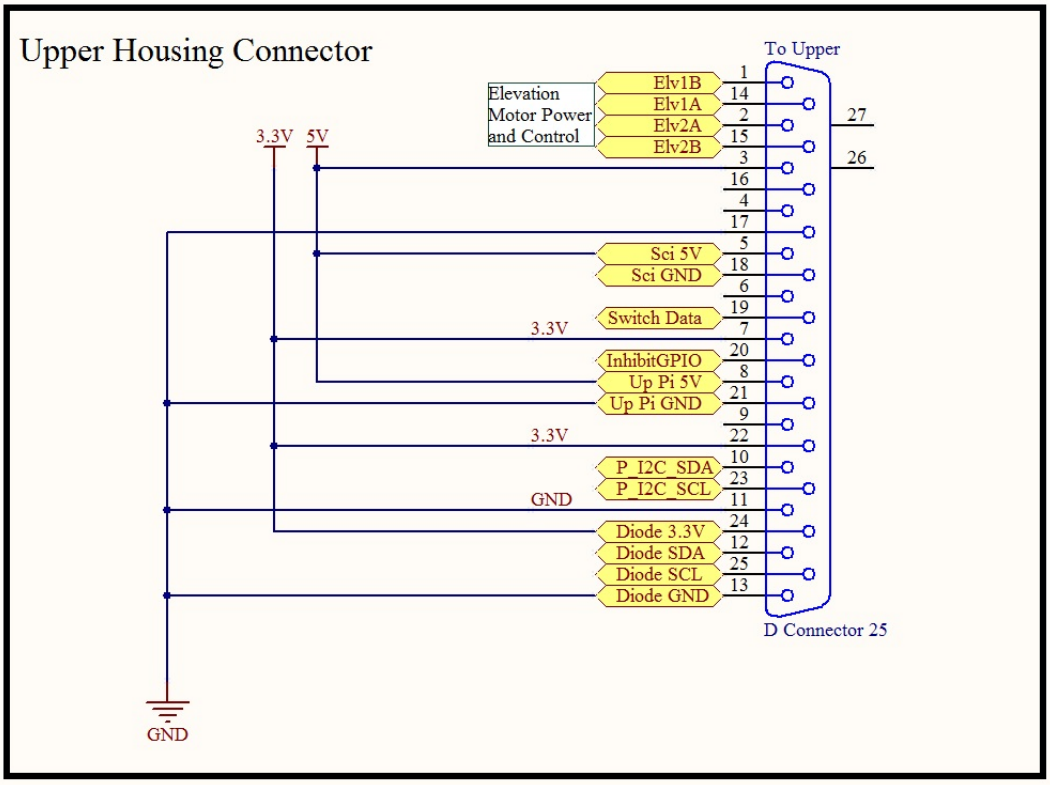
Upper Housing Connector
To Upper
Elevation
Motor Power
and Control
Elv1B
Elv1A
Elv2A
Elv2B
3.3V
5V
Sci 5V
Sci GND
Switch Data
InhibitGPIO
Up Pi 5V
Up Pi GND
P_I2C_SDA
P_I2C_SCL
Diode 3.3V
Diode SDA
Diode SCL
Diode GND
GND
D Connector 25

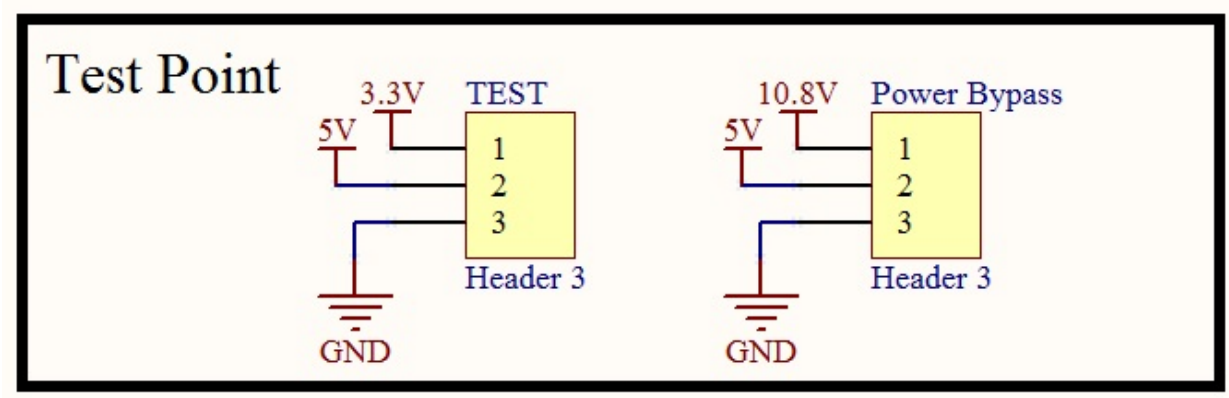
Test Point
3.3V
TEST
5V
1
2
3
Header 3
GND
10.8V
Power Bypass
5V
1
2
3
Header 3
GND

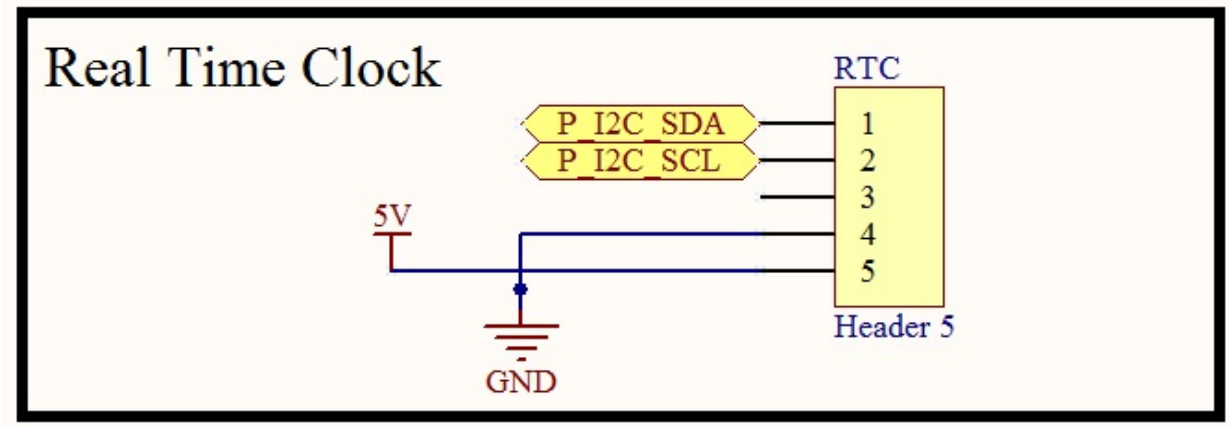
Real Time Clock
RTC
P_I2C_SDA
P_I2C_SCL
5V
1
2
3
4
5
Header 5
GND

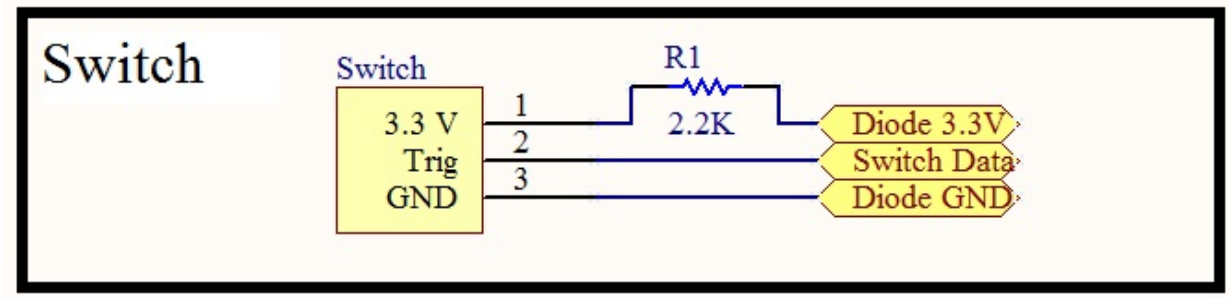
Switch
Switch
3.3 V
Trig
GND
1
2
3
R1
2.2K
Diode 3.3V
Switch Data
Diode GND

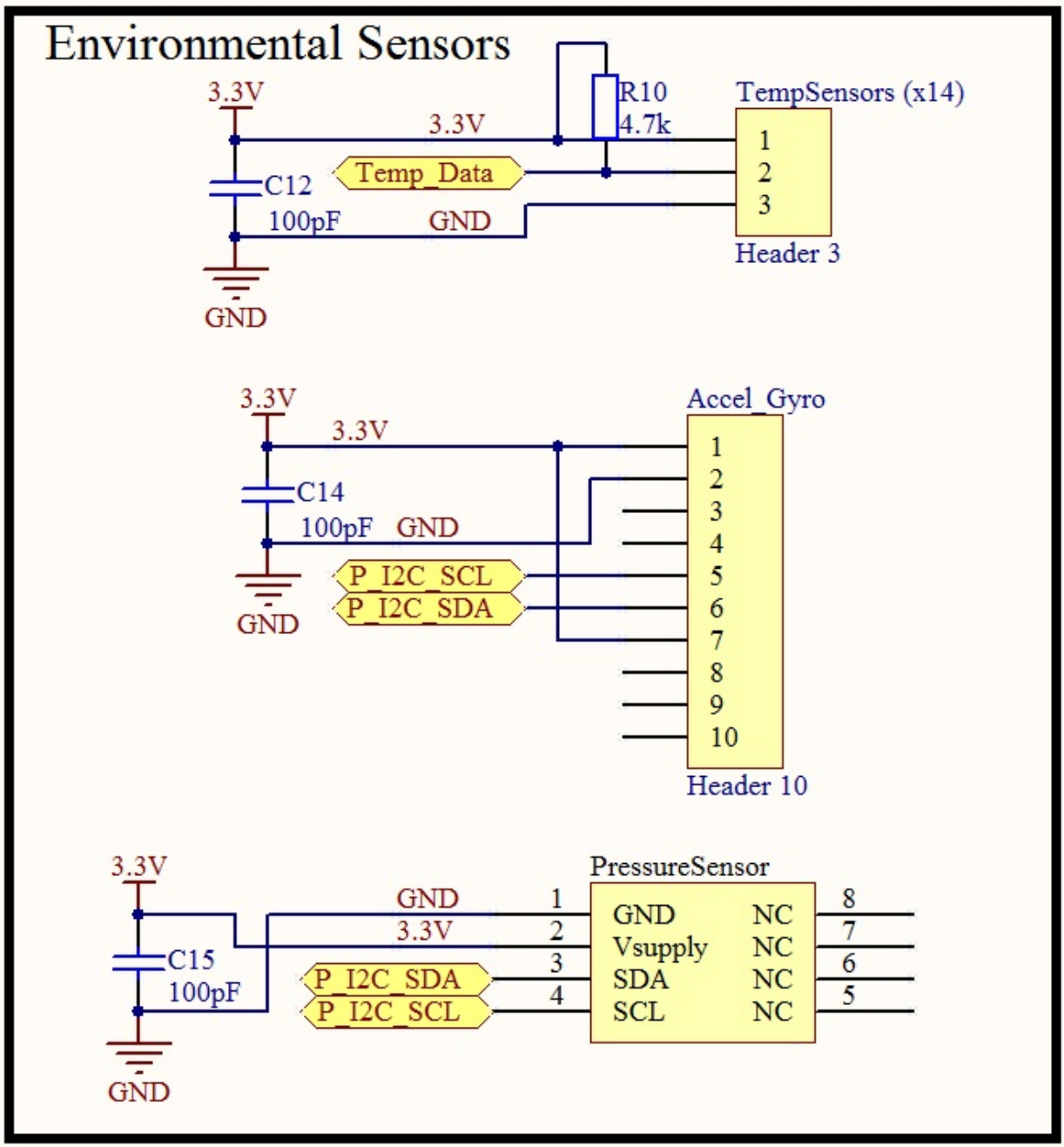
Environmental Sensors
3.3V
3.3V
R10
4.7k
TempSensors (x14)
1
2
3
Temp_Data
C12
100pF
GND
GND
Header 3
3.3V
3.3V
Accel_Gyro
1
2
3
4
5
6
7
8
9
10
C14
100pF
GND
P_I2C_SCL
P_I2C_SDA
GND
Header 10
3.3V
PressureSensor
GND
3.3V
C15
100pF
P_I2C_SDA
P_I2C_SCL
1
2
3
4
GND
Vsupply
SDA
SCL
NC
NC
NC
NC
8
7
6
5
GND

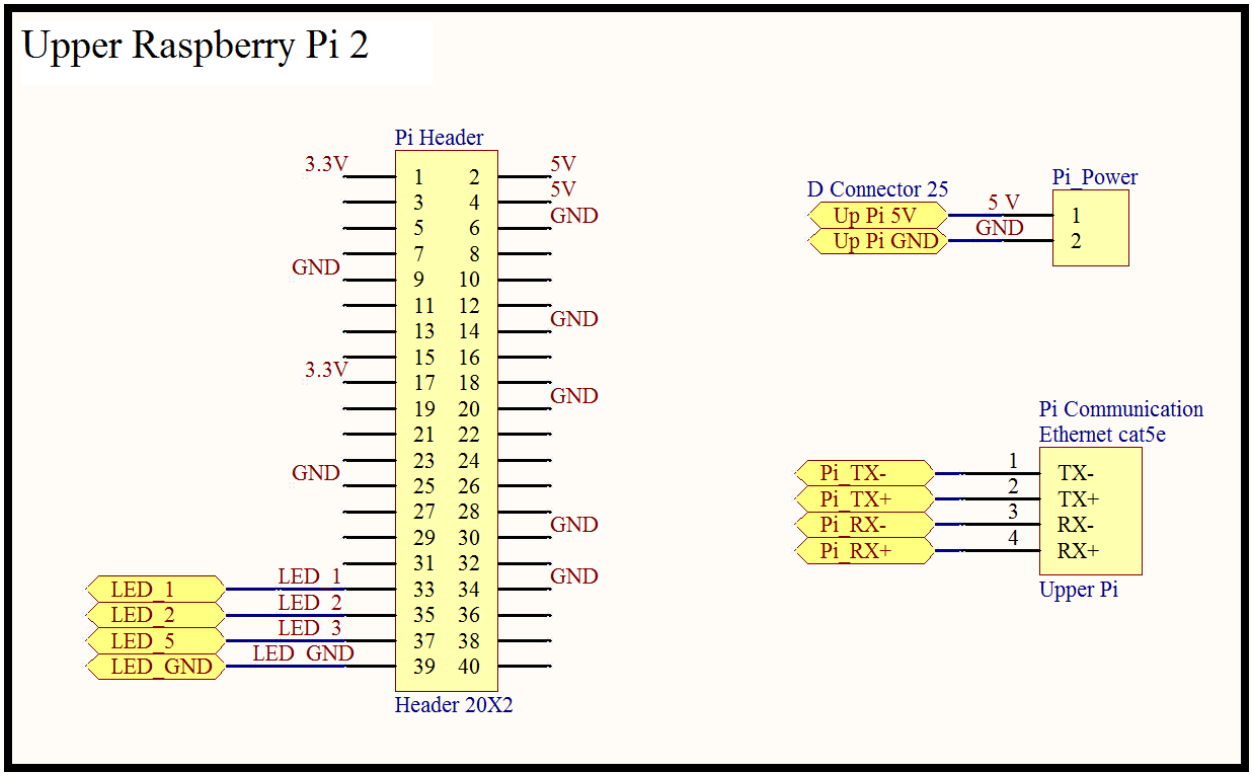
Upper Raspberry Pi 2
Pi Header
3.3V
5V
5V
GND
GND
GND
3.3V
GND
GND
GND
GND
1 2
3 4
5 6
7 8
9 10
11 12
13 14
15 16
17 18
19 20
21 22
23 24
25 26
27 28
29 30
31 32
33 34
35 36
37 38
39 40
LED_1
LED_2
LED_5
LED_GND
LED_1
LED_2
LED_3
LED_GND
Header 20X2
D Connector 25
Up Pi 5V
Up Pi GND
5 V
GND
Pi_Power
1
2
Pi Communication
Ethernet cat5e
Pi_TX-
Pi_TX+
Pi_RX-
Pi_RX+
1
2
3
4
TX-
TX+
RX-
RX+
Upper Pi

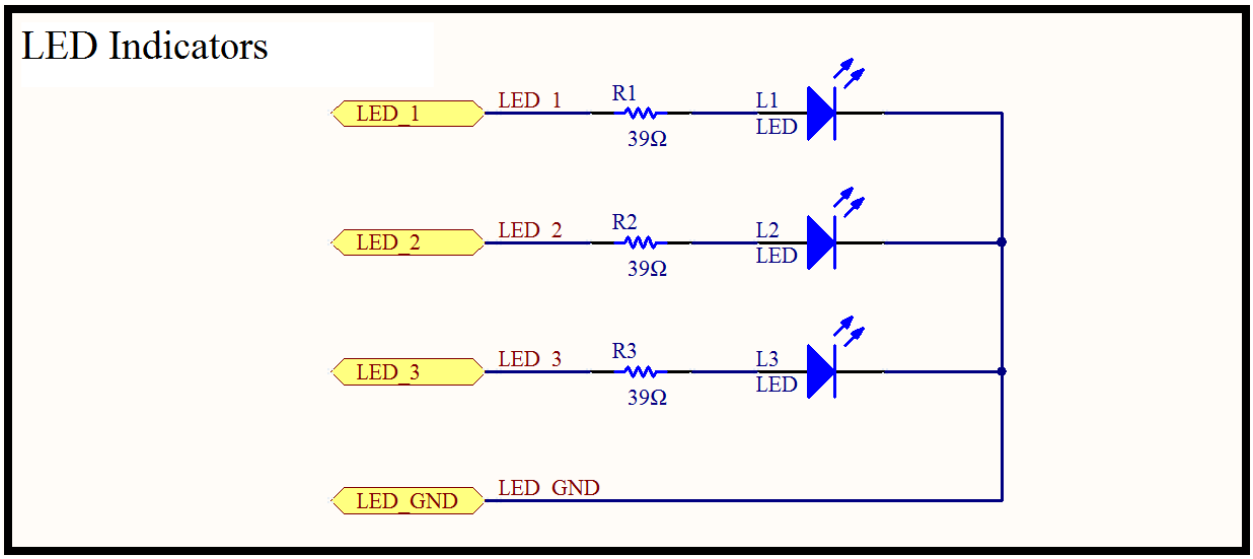
LED Indicators
LED_1
LED_1
R1
39Ω
L1
LED
LED_2
LED_2
R2
39Ω
L2
LED
LED_3
LED_3
R3
39Ω
L3
LED
LED_GND
LED_GND

C. Team Demographics

Student	Gender	Ethnicity	Race	Student Status	Disability
Paige Arthur	Female	non-Hispanic	Caucasian	Undergraduate	No
Dawson Beatty	Male	non-Hispanic	Caucasian	Undergraduate	No
Michael Catchen	Male	non-Hispanic	Caucasian	Undergraduate	No
Emma Cooper	Female	non-Hispanic	Caucasian	Undergraduate	No
Ryan Cutter	Male	non-Hispanic	Caucasian	Undergraduate	No
Haleigh Flaherty	Female	non-Hispanic	Caucasian	Undergraduate	No
Joseph Frank	Male	non-Hispanic	Caucasian	Undergraduate	No
Gage Froelich	Male	non-Hispanic	Caucasian	Undergraduate	No
Daniel Green	Male	non-Hispanic	Caucasian	Undergraduate	No
Rebekah Haysley	Female	non-Hispanic	Caucasian	Undergraduate	No
Ross Kloetzel	Male	non-Hispanic	Caucasian	Undergraduate	No
Alex Mulvaney	Male	non-Hispanic	Caucasian	Undergraduate	No
Virginia Nystrom	Female	non-Hispanic	Caucasian	Undergraduate	No
Samantha Palma	Female	non-Hispanic	Caucasian	Undergraduate	No
Severyn Polakiewicz	Male	non-Hispanic	Caucasian	Undergraduate	No
Erin Shimoda	Female	non-Hispanic	Caucasian	Undergraduate	No
Colin Sullivan	Male	non-Hispanic	Caucasian	Undergraduate	No
Logan Thompson	Male	non-Hispanic	Caucasian	Undergraduate	No

D. HASP Longitudinal Tracking

Name	Degree	Location/Current Employer
Cooper Benson	BS Aero Undergrad May 2016	Lockheed Martin
Brandon Boiko	ME Graduate BS May 2016	In Aerospace Industry
Jorge Cervantes	BS Aero 2016	MS candidate currently at CU Boulder
Becca Lidval	BS Aero May 2016	MS candidate currently at CU Boulder
Kamron Medina	Graduate may 2016	Roccor, small Aerospace company

E. References

Orion. Product Manuals Free Lifetime Tech Support 4.1" ID Orion Deluxe Safety Film Solar Filter. 2016. Web. June 2016.

"USB 3.0, USB 2.0, Gige, Firewire 800, Firewire 400 Industrial Cameras". Theimagingsource.com. N.p., 2016. Web. June 2016

F. Publications

Dawson Beatty, Haleigh Flaherty, Ross Kloetzel, Virginia Nystrom. *HELIOS V*. Presentation and Paper, April 2016. COSGC Symposium.

Dawson Beatty, Haleigh Flaherty, Ross Kloetzel, Virginia Nystrom. *HELIOS V*. Poster, October 2016. AIAA-RM Annual Technical Symposium.